2011

A loess–paleosol record of climate and glacial history over the past two glacial–interglacial cycles (~150 ka), southern Jackson Hole, Wyoming

Kenneth L. Pierce

Daniel R. Muhs

Maynard A. Fosberg

Shannon A. Mahan

Joseph G. Rosenbaum

See next page for additional authors

Authors

Kenneth L. Pierce, Daniel R. Muhs, Maynard A. Fosberg, Shannon A. Mahan, Joseph G. Rosenbaum, Joseph M. Licciardi, and Milan J. Pavich

Quaternary Research 76 (2011) 119–141

Contents lists available at ScienceDirect

Quaternary Research

journal homepage: www.elsevier.com/locate/yqres

A loess–paleosol record of climate and glacial history over the past two glacial–interglacial cycles (~150 ka), southern Jackson Hole, Wyoming

Kenneth L. Pierce [a,*], Daniel R. Muhs [b], Maynard A. Fosberg [c], Shannon A. Mahan [d], Joseph G. Rosenbaum [b], Joseph M. Licciardi [e], Milan J. Pavich [f]

[a] US Geological Survey, 2327 University Way, Box 2, Bozeman, MT 59715, USA
[b] US Geological Survey, MS 980, Box 25046 Denver Federal Center, Denver, CO 80225, USA
[c] Soil and Land Resources Division, Box 442339, University of Idaho, Moscow, ID 83844-2339, USA
[d] US Geological Survey, MS 974, Box 25046 Denver Federal Center, Denver, CO 80225, USA
[e] Department of Earth Sciences, University of New Hampshire, Durham, NH 03824, USA
[f] US Geological Survey, 955 National Center, Reston, VA 20192, USA

ARTICLE INFO

Article history:
Received 16 November 2010
Available online 19 May 2011

Keywords:
Loess
Paleosols
Bull Lake
MIS-3
MIS-4
MIS-6
Thermoluminescence
Meteoric Be-10
Cosmogenic Be-10
Jackson Hole

ABSTRACT

Loess accumulated on a Bull Lake outwash terrace of Marine Oxygen Isotope Stage 6 (MIS 6) age in southern Jackson Hole, Wyoming. The 9 m section displays eight intervals of loess deposition (Loess 1 to Loess 8, oldest), each followed by soil development. Our age-depth model is constrained by thermoluminescence, meteoric ^{10}Be accumulation in soils, and cosmogenic ^{10}Be surface exposure ages. We use particle size, geochemical, mineral-magnetic, and clay mineralogical data to interpret loess sources and pedogenesis. Deposition of MIS 6 loess was followed by a tripartite soil/thin loess complex (Soils 8, 7, and 6) apparently reflecting the large climatic oscillations of MIS 5. Soil 8 (MIS 5e) shows the strongest development. Loess 5 accumulated during a glacial interval (~76–69 ka; MIS 4) followed by soil development under conditions wetter and probably colder than present. Deposition of thick Loess 3 (~43–51 ka, MIS 3) was followed by soil development comparable with that observed in Soil 1. Loess 1 (MIS 2) accumulated during the Pinedale glaciation and was followed by development of Soil 1 under a semiarid climate. This record of alternating loess deposition and soil development is compatible with the history of Yellowstone vegetation and the glacial flour record from the Sierra Nevada.

Published by Elsevier Inc. on behalf of University of Washington.

Introduction

Overview

Loess–paleosol sequences are now recognized as one of the most complete terrestrial records of glacial–interglacial cycles of the Quaternary Period (Porter, 2001; Muhs and Bettis, 2003). In the contiguous U.S., loess is found in several broadly defined zones (Fig. 1). Loess covers much of the Mississippi River Valley, where it is derived from meltwater-transported silts of the Laurentide ice sheet (Bettis et al., 2003). In the Great Plains, west of the Mississippi River Valley, loess has both a glaciogenic and non-glaciogenic origin (Aleinikoff et al., 1999, 2008). Farther west, loess is widely distributed in southeastern Idaho (Lewis and Fosberg, 1982; Pierce et al., 1982; Scott, 1982), although its origins are not well understood. In and near southeastern Washington, loess of the Palouse region is glaciogenic, related to catastrophic flood deposits of proglacial Lake Missoula (Busacca et al., 2004).

In addition to these large loess regions, there are more restricted areas of loess in parts of North America. One of these, separated from the Idaho loess by the Teton Range, is a remarkable accumulation of loess along the upper Snake River in Jackson Hole, northwestern Wyoming (Fig. 2). In southern Jackson Hole, loess locally more than 8 m thick is distributed along both sides of the Snake River. We studied a thick section of loess and intercalated paleosols near Porcupine Creek, on a high outwash terrace in southern Jackson Hole (Figs. 3, 4). Collectively, the loess deposits and paleosols represent an unusually detailed record of environmental and climatic change spanning the last glacial–interglacial cycle (last 150 ka). Dated records covering this time interval are rare for the Rocky Mountain region, particularly the penultimate interglacial period and the earlier part of the last glacial period. The detail preserved in the Porcupine Creek section results from substantial loess deposition on a nearly horizontal outwash terrace, where erosion by water and wind was minimal due to low gradients and a probable dense vegetation cover.

The 9 m section has eight loess units separated by soils. The base of the section is a Bull Lake terrace gravel correlated with Bull Lake

* Corresponding author. Fax: +1 406 994 6556.
E-mail address: kpierce@usgs.gov (K.L. Pierce).

0033-5894/$ – see front matter. Published by Elsevier Inc. on behalf of University of Washington.
doi:10.1016/j.yqres.2011.03.006

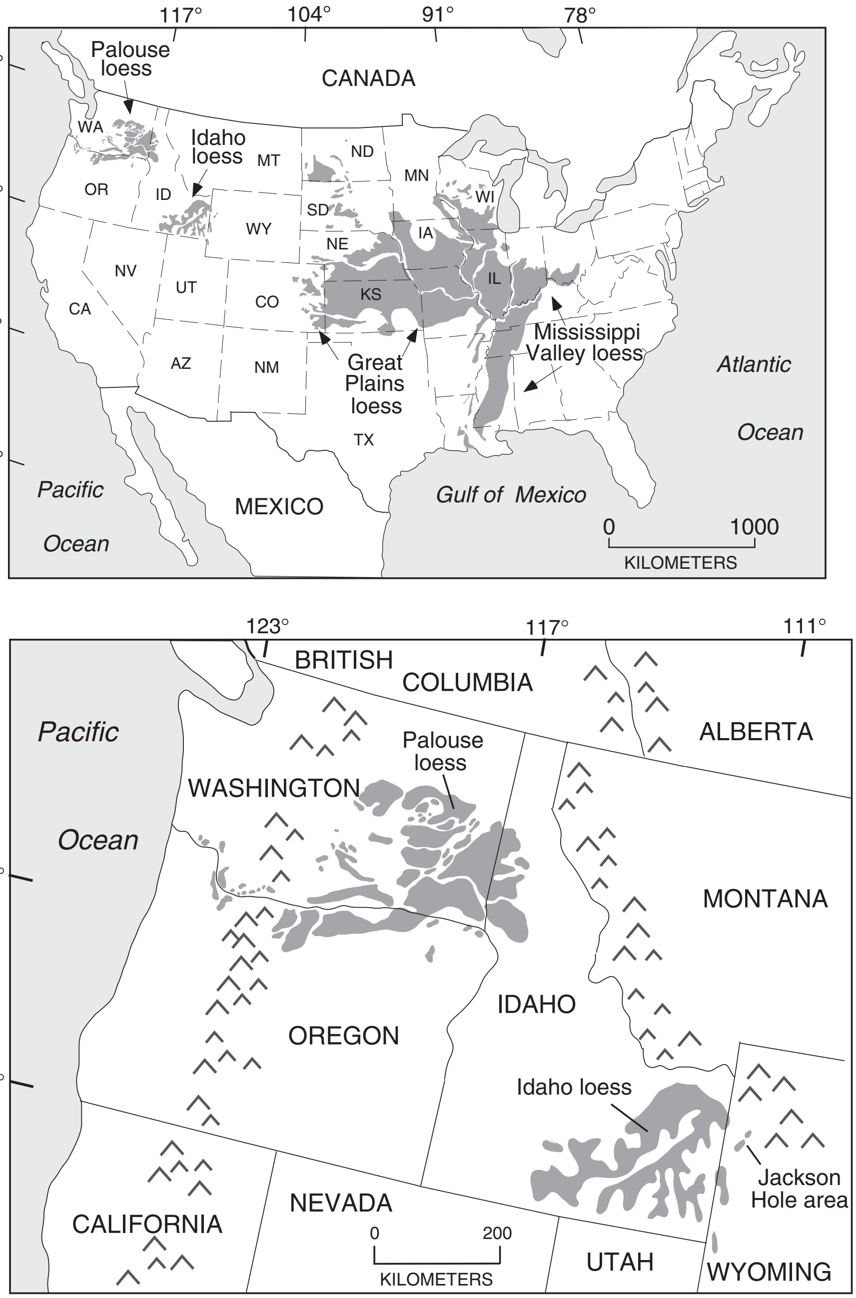

Figure 1. Upper: map showing the distribution of loess in the U.S., outside of Alaska, and location of the Idaho loess province. Compiled from Bettis et al. (2003), Busacca et al. (2004), and sources therein. Lower: map of the northwestern U.S., showing the Palouse loess province (redrawn from Busacca et al., 2004), Idaho loess province, and location of the Jackson Hole area.

moraines on which glacial boulders have a median oldest boulder age of 154 ± 5 ^{10}Be ka (Licciardi and Pierce, 2008). From the surface to a depth of 7 m, six stratigraphically consistent thermoluminescence (TL) ages extend back to ~76 ka. The lowest 1.5 m of the section is bracketed between ~154 ka and ~76 ka and consists of a buried loess and soil complex (Units, 6, 7, and 8). The interpolation of ages for this loess and soil complex is based on buildup through time of meteoric ^{10}Be in these three units. In addition to the field description and particle size distribution, we use geochemistry, mineral magnetic analysis, and clay mineralogy to interpret loess and soil character changes. The backhoe pits were sampled in 1994 and TL and ^{10}Be analysis done before 2000. Optically stimulated luminescence (OSL; see review in Duller, 2004) is now preferred over TL for most eolian sediments, but the samples are no longer available for analysis and re-excavation of the site is not possible due to funding and access issues. In this report, references to non-U.S. Department of Interior (DOI) products do not constitute an endorsement by DOI. Supplements to this report are: 1) Stratigraphy and soil horizons of the composite Porcupine Creek loess section, southern Jackson Hole, Wyoming, and 2) Table of soil-loess horizons showing particle sizes (4), organic carbon, calcium carbonate, major element oxides (10), trace elements (6) and magnetic properties (4) of the Porcupine Creek loess section, southern Jackson Hole, Wyoming.

Study area: climate, vegetation, and soils

Jackson Hole is a north-south-trending valley in northwestern Wyoming, situated between the Yellowstone Plateau to the north, the Teton Range to the west, the Absaroka Range to the far northeast, the Wind River Range to the far east, and the Gros Ventre Range to the east (Figs. 2, 3). After exiting Jackson Lake, the Snake River flows

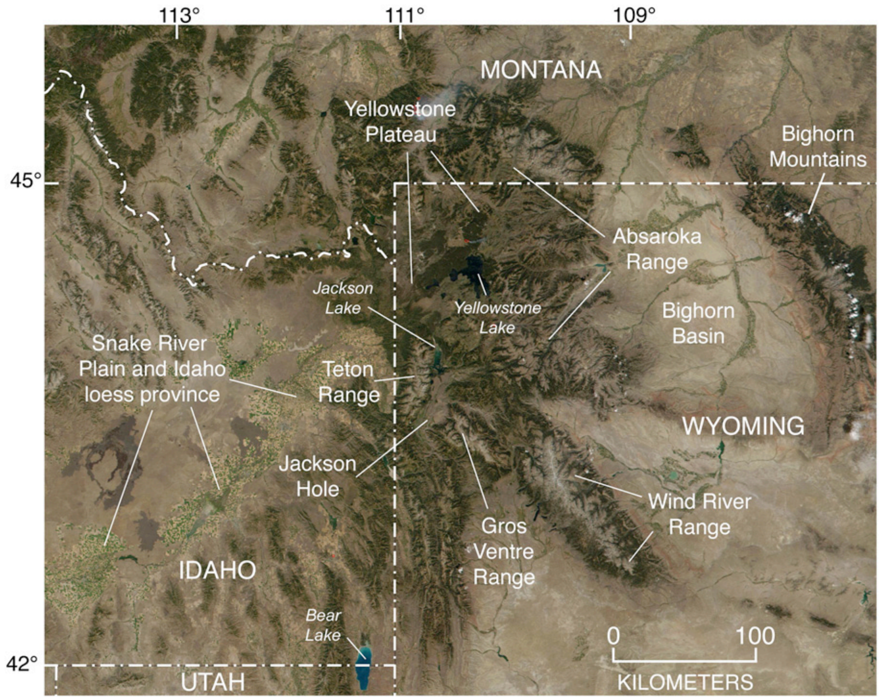

Figure 2. Natural-color moderate-resolution imaging spectroradiometer (MODIS) image from the Terra satellite of northwestern Wyoming, southern Montana, and southeastern Idaho, showing study area and other localities referred to in the text. The agricultural areas in southern Idaho, obvious as alternating tan and green speckled areas, represent the loess-covered areas. Image taken August, 2001 and is used through the courtesy of Jacques Descloitres, MODIS Land Rapid Response Team at NASA GSFC.

south along the valley axis, which has an altitude of ~2100 m in its northern part and ~1850 m in its southern part. Tributaries to the Snake River drain Quaternary rhyolites and minor basalts from the Yellowstone Plateau, Precambrian quartz monzonites and gneisses in the Teton Range, Tertiary andesites from the Absaroka Range, and Mesozoic sandstones and shales bordering the east side of Jackson Hole.

The climate of Jackson Hole is continental, with cold winters and warm summers. At the Porcupine Creek section (altitude 1926 m) mean annual precipitation is estimated to be 53 cm (19.5 in.) and mean annual temperature is 4°C (Phil Farnes, Snowcap Hydrology, formerly NRCS, written commun., 2002). Productive hay crops now grow at the study site. At nearby sites northerly slopes have patchy forests of conifers and aspens. A deep wetting cycle associated with spring snow melt is an important factor in the growth of lush grass and forbs, and also deep soil development with leaching and redeposition of carbonate in the modern surface soil.

Vegetation in the Yellowstone–Grand Teton–Jackson Hole area (Fig. 5) is strongly conditioned by elevation (Baker, 1986; Despain, 1990; Whitlock, 1993). On the floor of Jackson Hole, precipitation increases both to the west and to the north. Below ~1800 m elevation, vegetation is dominated by sagebrush (*Artemisia* spp.) and grass (Gramineae) steppe. The vegetation at the Porcupine Creek loess section is the habitat type "*Artemisia vaseyana*/*Festuca idahoensis*" (mountain big sagebrush/Idaho fescue) (Hironaka et al., 1983). Other plant species present are *Artemisia tridenta* ssp. *tripartite* (three tip sagebrush) and *Symphoricarpos occidentalis* (snowberry). Forest is found above the sagebrush–grassland steppe, and dominant tree species in five forest zones are, at successively higher elevations: (1) limber pine (*Pinus flexilis*); (2) Douglas fir (*Pseudotsuga menziesii*) with subordinate limber pine and quaking aspen (*Populus tremuloides*); (3) lodgepole pine (*Pinus contorta*), with Engelmann spruce (*Picea engelmannii*) and subalpine fir (*Abies lasiocarpa*) in the upper part of this zone; (4) a mixture of dominant spruce (*P. engelmannii*) and fir (*A. lasiocarpa*), with subordinate whitebark pine (*Pinus albicaulis*) and lodgepole pine (*P. contorta*); and finally (5) whitebark pine (*P. albicaulis*). Above the highest forest zone at ~2900 m elevation, alpine tundra is dominated by grasses (Gramineae), sedges (Cyperaceae), and rushes (Juncaceae).

Surface soils in the region are influenced by the dominant vegetation (Young, 1982). Above treeline, soils under tundra are Cryorthents or Haplocryolls with minimally developed profiles (Fig. 5). At high elevations in the spruce–fir forest of the Teton Range, the main soils on flat surfaces or gentle slopes are Cryorthents or Inceptisols (Dystrochrepts) with O/E/Bw/C profiles. At lower elevations in lodgepole pine forest of the Teton Range, soils on flat areas or gentle slopes are Alfisols (Haplocryalfs) with O[A]/E/Bt/C profiles or Inceptisols (Haplocryepts) with O/E/Bw/C[R] profiles. Finally, at low elevations in Jackson Hole itself, under sagebrush–grassland steppe, soils are Mollisols (Haplocryolls) with A/Bw/C or A/Bw/Bk/C profiles: a Bt may be locally present (Argicryolls). The modern surface soil at the top of the Porcupine Creek section is a Mollisol (Argicryoll) with an A/Bt/Bk/C profile.

Idaho–western Wyoming loess province

Loess is extensive over much of southeastern Idaho and adjacent parts of western Wyoming (Fig. 1). Loess in this region is important for the irrigated and productive farms along and adjacent to the Snake River Plain (Lewis and Fosberg, 1982). The age of loess extends well back into the Quaternary and locally contains the 639 ± 2 ka Lava Creek B ash (tephra) (Izett and Wilcox, 1982; Lamphere et al., 2002). Loess occurs on the margins of and within the eastern Snake River Plain and total thickness varies considerably, in part as a function of the age of the substrate (Scott, 1982).

In a study of ten stratigraphic sections along the eastern Snake River Plain, Pierce et al. (1982) informally divided the upper part of the loess into loess unit A (younger) and loess unit B (older) separated by a buried soil that is more strongly developed than the surface soil. Based on dated volcanic rocks and glacial deposits, these workers concluded that loess unit A was deposited between ~70 and 10 ka, the

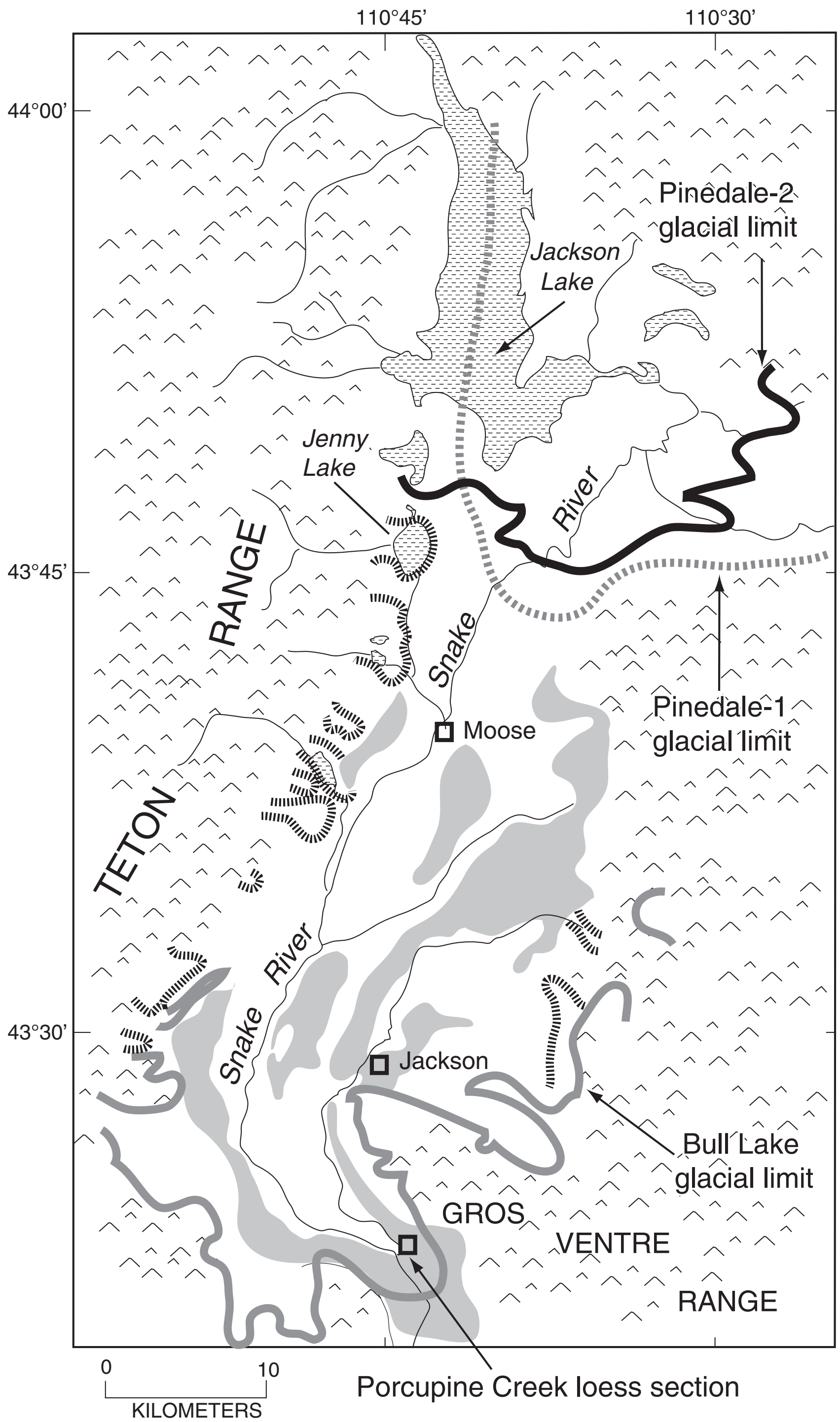

Figure 3. Map of the Jackson Hole area, showing distribution of loess (gray shaded areas; compiled from Young, 1982 and Glenn et al., 1983), and the location of the Porcupine Creek loess section. Also shown are the locations of moraines that mark the limits of Bull Lake, Pinedale-1, and Pinedale-2 glacial advances from the Yellowstone Plateau–Absaroka Range area (Pierce and Good, 1992; Love et al., 2007; Licciardi and Pierce, 2008). Much of the blank area is glacial outwash plain whose seasonal deflation generated Pleistocene loess deposits. Black dashed/gray lines outline Pinedale end moraines deposited by valley glaciers from the Teton Range and Gros Ventre Range.

prominent buried soil formed between ~70 and 130 ka, and loess unit B was deposited before ~130 ka.

For the eastern Snake River Plain at the Idaho National Laboratory, Forman et al. (1993) concluded that a clay-rich interval within dated loess deposits was equivalent to the buried soil separating loess units A and B of Pierce et al. (1982), and therefore that loess unit B dated roughly to 70–80 ka. Dechert et al. (2006) argued that this clay-rich interval was an alluvial deposit within loess unit A rather than a buried Bt horizon 1.5 m thick. Scott (1982) mapped this low area as a playa deposit, thus suggesting the presence of fine-grained alluvium.

Loess in the Jackson Hole area

Jackson Hole is adjacent to the extensive Idaho loess province that extends to the west side of the Teton Range just west of Jackson Hole (Fig. 1). Compared to Idaho, much less attention has been paid to loess in western Wyoming, but some basic characteristics are known.

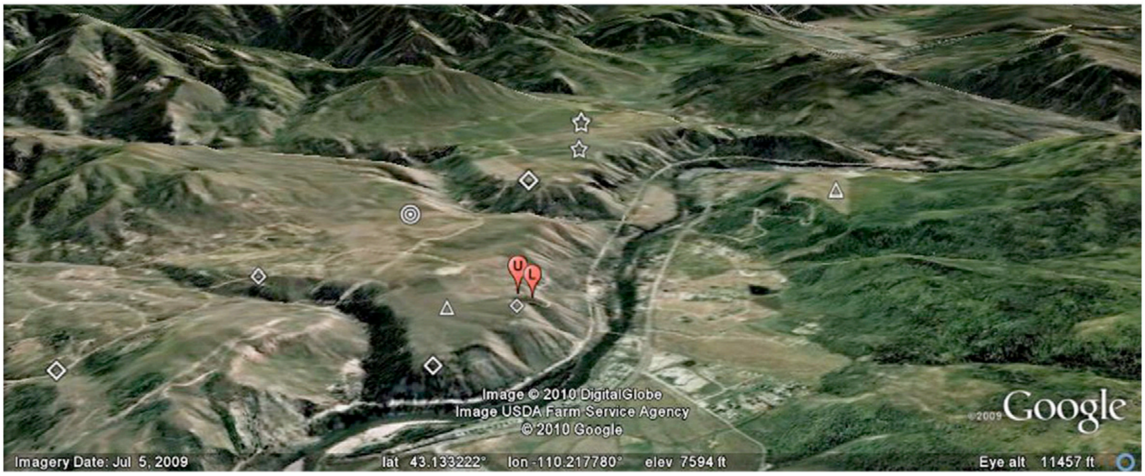

Figure 4. View of southern Jackson Hole showing the setting of the Porcupine Creek loess section. Balloons indicate sites of upper (U) and lower (L) pits. Diamonds are sites where a calcic Bk horizon were observed near boundary of loess on Bull Lake gravel, including the diamond just left of lower middle where a cemented Bca horizon 1.1 m thick was observed. Triangles and stars indicate Bull Lake outwash terrace and moraines, respectively. Bull's eye is the location of a glacial depression. The Snake River flows away from viewer. Three dimensional image downloaded from Google.

Gently sloping landforms such as outwash terraces of pre-Pinedale age commonly have thick loess deposits (Love et al., 1992). A north-south transect of Jackson Hole by Glenn et al. (1983) shows that the loess source was probably to the north, as indicated by southward decrease in both mean particle size and sand content. Glenn et al. (1983) also found the sand content of Jackson Hole loess to be higher than that west of the Teton Range. This finding also supports a local Jackson Hole outwash source. Modern winds in central Jackson Hole are commonly from the south to south-southwest; winds are almost as common but not as strong from the north (wind data are courtesy of the Western Regional Climate Center, Desert Research Institute, Reno, Nevada [http://www.raws.dri.edu/cgi-bin/rawMAIN.pl?wyW-GRA; accessed on 19 January 2010]). Glenn et al. (1983) concluded that in glacial times winds were from the north and most likely from katabatic (cold air) winds descending from the greater Yellowstone glacial system. Such an origin of loess via deflation of locally dry outwash plains by katabatic winds probably also produced loess deposits in southern Alaska (Rieger and Juve, 1961) and central Alaska (Thorson and Bender, 1985; Muhs and Budahn, 2006).

Loess in Jackson Hole has mineralogy similar to loess found in other regions. Glenn et al. (1983) reported that the dominant minerals in the coarse silt fraction are, in decreasing order of abundance: K-feldspar (31–43%), quartz, including chalcedony (18–40%), plagioclase (3–13%), and calcite (1–13%). Vermiculite, muscovite, hornblende, chlorite, glass, kyanite, pyroxene, and garnet were also identified in some samples, in amounts of 5% or less.

We hypothesize that deposition of at least the thicker loess units at the Porcupine Creek section is related to the glacial outwash history of the area. During the last (Pinedale) glaciation, outlet glaciers from the greater Yellowstone glacial system advanced first from the northeast and then the north into Jackson Hole (Fig. 3). Meltwaters from these ice bodies deposited extensive outwash covering most of the floor of Jackson Hole (Love et al., 1992; Pierce and Good, 1992; Love et al., 2007). Such outwash is the likely source of the silt that forms the bulk of the Jackson Hole loess deposits (Fig. 3). Thus, as background for testing the hypothesis of loess derivation from local glaciogenic sources, we will review the glacial history of the area.

Glacial history

During the last two Rocky Mountain glaciations (Bull Lake and Pinedale), glacial ice on the southern part of the greater Yellowstone ice mass advanced into Jackson Hole (Fig. 3) where it was joined by local mountain valley glaciers from the Teton Range and other ranges. During the Bull Lake glaciation, a large glacier flowed south from Yellowstone and occupied essentially all of Jackson Hole, terminating about 4 km down-valley (south) of the Porcupine Creek section (Fig. 3). The Pinedale glaciation was considerably more restricted in this region, as indicated by terminal moraines that mark a Pinedale maximum extent ~50 km up-valley (north) from the Bull Lake ice limit in southern Jackson Hole (Pierce and Good, 1992).

The Bull Lake moraines of Jackson Hole have physical characteristics that are consistent with Bull Lake moraines recognized elsewhere in the Rocky Mountains. Boulders on the moraines exhibit signs of weathering and the morainal ridge morphology can still be recognized in places, but the rather thick loess cover in Jackson Hole commonly subdues the ridge expression. In the northern reaches of Jackson Hole, recessional Bull Lake deposits are characterized by a thick loess mantle with a prominent reddish buried soil near the base of the loess. In contrast, Pinedale deposits in the Jackson Hole area lack a distinct loess cover (Young, 1982; Pierce and Good, 1992).

Inside the Bull Lake morainal loop at the southern end of Jackson Hole is an outwash terrace ~120 m above the Snake River, upon which the loess of the Porcupine Creek section accumulated (Fig. 3). Subdued Bull Lake moraines occur down valley on the same high terrace bench, supporting correlation of the outwash gravel at the base of the Porcupine Creek section with the Bull Lake moraines (Figs. 3, 4).

About 6–10 km west of the Porcupine Creek section, the Bull Lake moraines are studded with large granitic boulders from the Teton Range that are appropriate for cosmogenic nuclide dating (Licciardi and Pierce, 2008). Excluding one young outlier, ^{10}Be exposure ages of boulders on these moraines have a mean age of 136 ± 13 ^{10}Be ka (n = 7) and a median "oldest boulder age" of 154 ± 5 ^{10}Be ka. These age constraints are consistent with age estimates for Bull Lake moraines on the west side of the greater Yellowstone glacial system near West Yellowstone, Montana (Richmond, 1964), which have an age of ~140 ka based on combined obsidian hydration and K–Ar methods (Pierce et al., 1976; Colman and Pierce, 1981; Pierce, 2004). These ages all fall within the later part of Marine Oxygen Isotope Stage 6 (MIS 6) which started ~190 ka and ended ~130 ka (Martinson et al., 1987). For comparison, we note that the MIS 6/5 boundary in the speleothem record at Devils Hole, Nevada, was independently dated by Winograd et al. (1997) at ~140 ka.

Dating of deposits from the Bull Lake type area 130 km east of Jackson Hole in the Wind River Range (Blackwelder, 1915; Fig. 2) also suggests that Bull Lake deposits formed during MIS 6. Pedogenic carbonate coats from two Bull Lake terraces yielded uranium series ages of 167 ± 6 ka and 150 ± 8 ka (Sharp et al., 2003). These uranium series ages are older than cosmogenic ^{36}Cl and ^{10}Be data that indicate

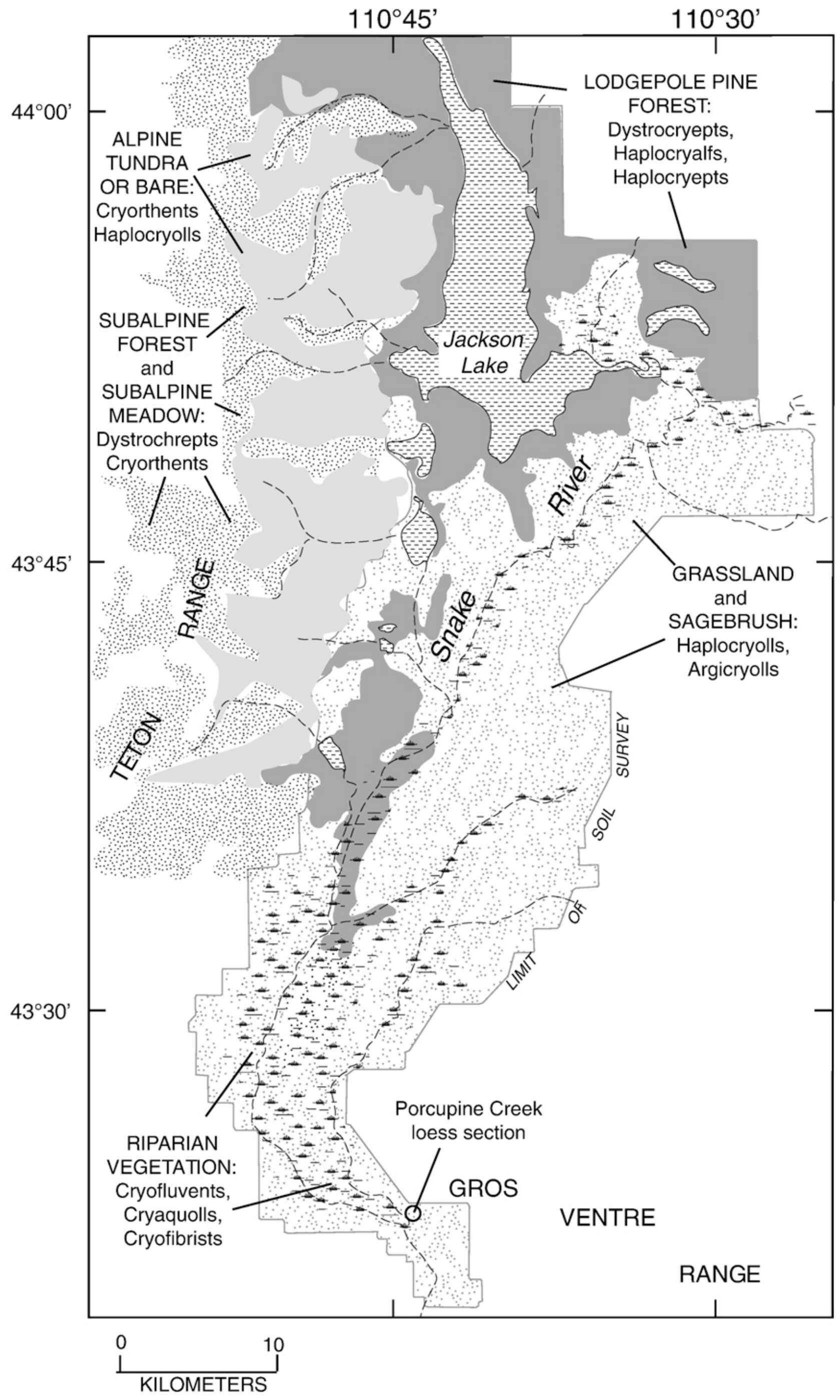

Figure 5. Map showing the distribution of major vegetation types and soils in the Jackson Hole area and surrounding mountains, compiled from Young (1982) and Wyoming Geographic Information Science Center (2007) (http://www.wygisc.uwyo.edu/atlas/).

a minimum exposure age of >130 ka for older Bull Lake moraines and a maximum age of 130–120 ka for younger moraines in the same type Bull Lake glacial sequence (Chadwick et al., 1997; Phillips et al., 1997); the cosmogenic ages at the type Bull Lake locality, especially the ^{36}Cl ages, may be anomalously too young (Sharp et al., 2003; Pierce, 2004).

The Pinedale glaciation is correlated with the last glacial period ("Wisconsin" of the mid-continental U.S.) equivalent to MIS 2 of Martinson et al. (1987). The start of the Pinedale is uncertain, and if they were present, moraines of MIS 3 age and MIS 4 age might also be classified as Pinedale in age.

Inside the Bull Lake glacial limit, Pinedale moraines of local valley glaciers occur on both valley walls of Jackson Hole (Fig. 3). Farther north, Pinedale moraines along the southern margin of the greater Yellowstone glacial system define three glacial stands: (1) Pinedale-1 (Burned Ridge) advance by glacial lobes from the east and northeast, but not from the north (i.e., not the Yellowstone Plateau area); (2) Pinedale-2 (Hedrick Pond) advance by glacial lobes from the north (Yellowstone Plateau) and the northeast; and (3) Pinedale 3 (Jackson Lake) phase by a retreat from the Pinedale 2 position (Pierce and Good, 1992; Love et al., 2007). The ages of Pinedale moraines and outwash deposits in the Yellowstone–Teton–Jackson Hole–Wind

River area have been estimated by a variety of methods, including radiocarbon, uranium-series, obsidian hydration rind thicknesses, weathering rind thicknesses, and cosmogenic nuclide surface exposure dating (Pierce et al., 1976; Pierce, 1979; Colman and Pierce, 1981; Chadwick et al., 1997; Phillips et al., 1997; Licciardi et al., 2001; Sharp et al., 2003; Licciardi and Pierce, 2008). Weathering rind thicknesses and U-series ages on gravels indicate that the earliest Pinedale advance in other locations (McCall, Idaho and the Wind River Range, Wyoming) could be as old as 50–70 ka and of early Wisconsin age (Colman and Pierce, 1981, 1986; Sharp et al., 2003). However, all workers in the region agree that the most recent ice advance of any significant extent was the Pinedale advance of late-Wisconsin age. Cosmogenic isotope measurements suggest that northern and eastern outlet glaciers of the greater Yellowstone glacial system reached their maximum positions at ~16–19 ka and began to retreat shortly thereafter (Licciardi and Pierce, 2008). Pinedale moraines at the mouth of one east-draining valley of the Teton Range are somewhat younger than those of the northern and eastern outlet glaciers of the Yellowstone ice cap. At Jenny Lake, for example (Fig. 3), ^{10}Be exposure ages of boulders on an outer moraine loop have a mean of 14.6 ± 0.7 ^{10}Be ka ($n = 10$) whereas boulder ages on an inner moraine enclosing the lake have a mean of 13.5 ± 1.1 ^{10}Be ka ($n = 9$) (Licciardi and Pierce, 2008). The Pinedale moraines in the Jackson Hole area lack a distinct loess cover (Young, 1982; Pierce and Good, 1992).

Methods

Sampling

The loess deposits are divided into eight units (Fig. 6) based on soils developed downward into each loess unit. A unit (i.e. 5) consists of a loess (Loess 5) and a soil developed in it (Soil 5). In this report these local terms (Unit, Loess, and Soil) are capitalized to make their stratigraphic designation apparent (Fig. 7, see Supplement 1).

The ~9 m section of loess was exposed in three backhoe pits along a transect extending from the upper flat terrace down across the top edge of the terrace scarp. (Lower pit 43.37391°N, 110.73557°W; upper pit 43.374235°N; 110.734825°W). A distinctive dark gray soil horizon (mollic horizon?) in the upper part of Soil 5, at ~6 m depth, served as a marker where it was exposed in the lower and middle pits and encountered by shallow augering in the bottom of the upper pit. The composite section described and sampled came entirely from the upper and lower pits, with the middle pit serving as the best place to obtain TL and radiocarbon ages from and just above dark gray A horizon of Soil 5 (see Supplement 1).

Soil analyses

Soils were described using standard USDA-NRCS procedures (Soil Survey Staff, 1993, 2010) and are described in Supplement 1. Soil

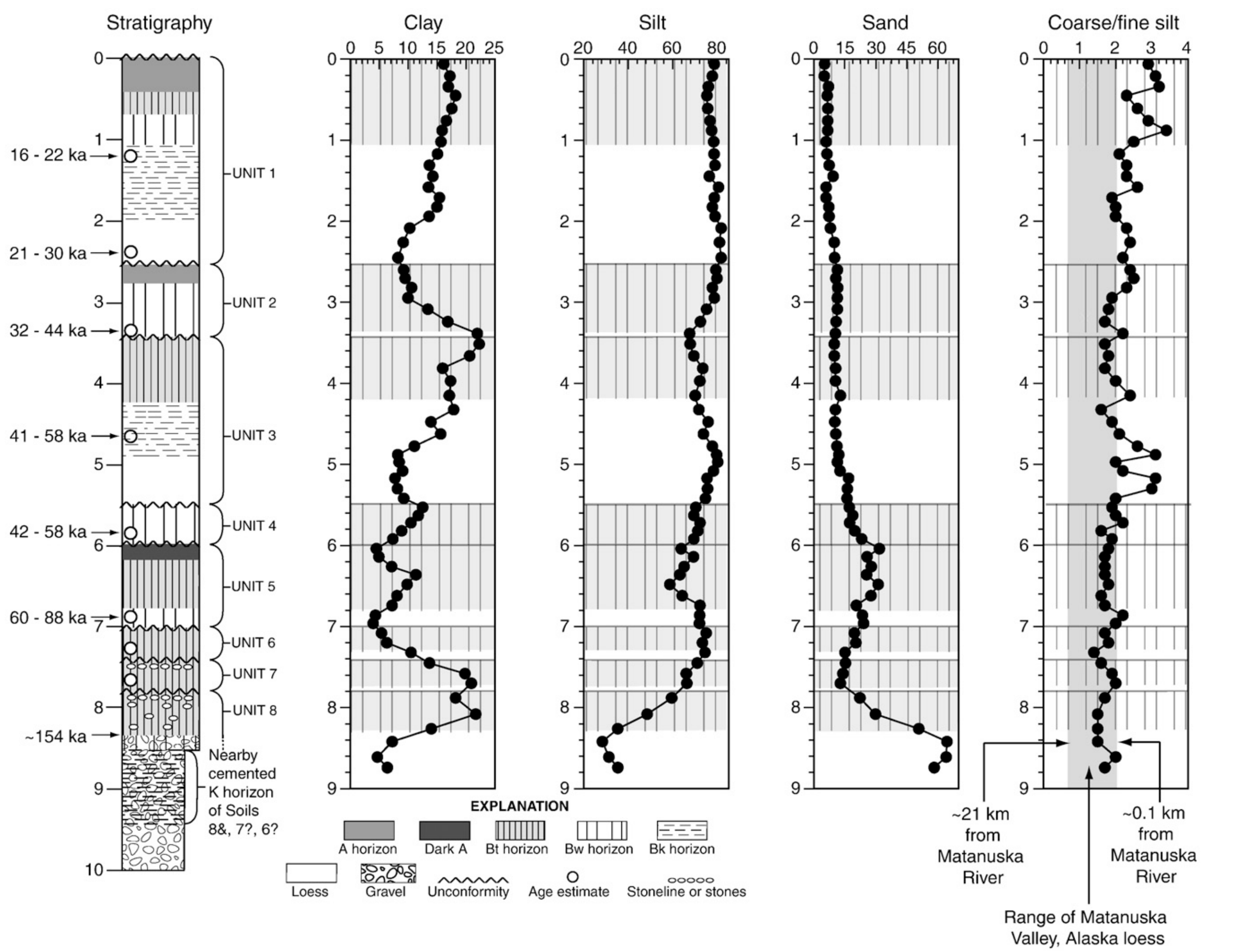

Figure 6. Stratigraphy of the Porcupine Creek loess section and plots of clay, silt, sand and the ratio of coarse to fine silt. The age ranges (ka) are based on one-standard deviation of the TL analysis calculated for combined 10% and 25% water content. The darker A horizon is the mollic horizon for Soil 5. For coarse/fine silt column, the shaded band is for Matanuska valley loess, Alaska (Muhs et al., 2004).

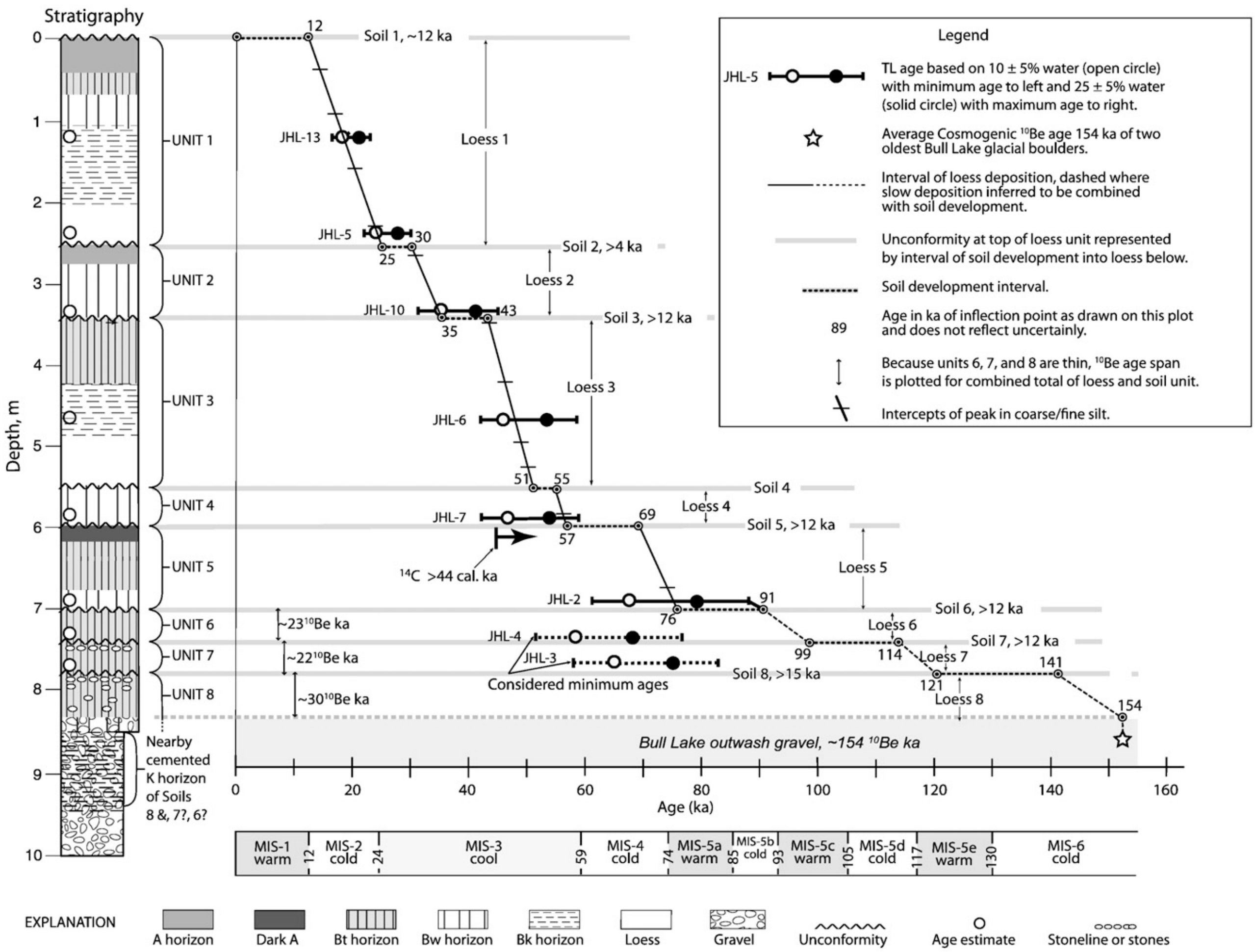

Figure 7. Chronology of the Porcupine Creek loess section. This age versus depth plot is constrained by: 1) cosmogenic ^{10}Be age of Bull Lake glacial boulders (~154 ± 5 ^{10}Be ka), 2) the upper six TL ages, 3), amounts of meteoric ^{10}Be accumulation, and 4) soil development estimates. The TL ages are plotted for both 10 ± 5% (open circles) and 25 ± 5% pore water (solid circles). On the lower left are time spans indicated by the accumulation of meteoric ^{10}Be for Soils 6–8 (Table 2). Along gray bands to right of age plot are minimum time spans estimated for development of each soil. For the mollic A horizon shown in black at the top of Unit 5, the bar and arrow is for the radiocarbon age considered a minimum of 44 cal ka BP (see text). The numbers at the inflection points are simply from the intercepts on this age plot to aid the reader: the actual age uncertainty is considerably greater. Marine oxygen isotope (MIS) timescale after Martinson et al. (1987).

analyses followed standard pedological methods which were used in other loess studies by Muhs et al. (2003). Particle-size analyses of the <2 mm fraction were done using sieve (53 μm) and pipette after removal of carbonates with HCl, destruction of organic matter with H_2O_2, and dispersion with Na-pyrophosphate. Organic matter content was determined by a modified Walkley–Black method and $CaCO_3$ content was determined using a Chittick apparatus. Major and trace element geochemistry was determined on bulk samples using wavelength-dispersive X-ray fluorescence. Mineralogy of the clay fraction was determined by X-ray diffraction (XRD) analysis. Prior to XRD analyses, samples received the same pretreatments as for particle size analyses. Clays were then separated by sedimentation and mounted on slides for X-ray analysis in three conditions: air-dried, glycolated, and heat-treated (550°C for one hour).

In addition to the meteoric ^{10}Be accumulation, the degree of soil development was used as a rough indicator of the magnitude of the time spans involved, although changes in climate are also a factor. The surface soil (Soil 1) on Loess 1 took about 12 ka to develop based on the time since recession of Pinedale glaciers and cessation of outwash (Pierce, 2004; Licciardi and Pierce, 2008). The surface soil has a weak Bt horizon so it was judged that any buried soil with a comparable, or stronger Bt horizon took at least 12 ka to develop.

Magnetism measurements

For magnetic mineralogical analyses of soils and loesses, methods followed those of Rosenbaum et al. (1996). Five magnetic mineralogical parameters are presented: (1) magnetic susceptibility (MS) measured at low frequency (600 Hz), essentially a measure of total ferrimagnetic mineral content (i.e., magnetite and maghemite); (2) anhysteretic remanent magnetization (ARM), also a measure of ferrimagnetic mineral content but more highly sensitive to extremely small (single-domain) grains (Dunlop and Özdemir, 1997); (3) "hard" isothermal remanent magnetization (HIRM), a measure of high-coercivity magnetic minerals, such as hematite; (4) frequency-dependent magnetic susceptibility (FDMS; the difference between MS measured at 600 and 6000 Hz); and (5) the ratio of anhysteretic remanent magnetization (ARM) to magnetic susceptibility (MS). The FDMS and ARM/MS values are measures of magnetic grain size, where higher values reflect higher proportions of ultra-fine (superparamagnetic) and slightly larger (single domain) grains, respectively.

Thermoluminescence dating

The samples were analyzed at the USGS Luminescence Dating Laboratory by Paula Maat (sample preparation and preliminary

Table 1
Thermoluminescence data and ages for the Porcupine Creek loess section.

A. Dosimetry data for loess samples. Listed in stratigraphic sequence.

Sample	Water[a] (%)	K (%)[b]	U (ppm)[b]	Th (ppm)[b]	Cosmic-ray component[c]	Dose rate (Gy/ka)[d]
JHL-13	.10 ± 0.05	1.60 ± 0.07	3.84 ± 0.54	8.39 ± 0.32	.272 ± 0.03	4.78 ± 0.19
	.25 ± 0.05	1.60 ± 0.07	3.84 ± 0.54	8.39 ± 0.32	.272 ± 0.03	4.12 ± 0.16
JHL-5	.10 ± 0.05	1.56 ± 0.07	3.52 ± 0.51	8.04 ± 0.31	.226 ± 0.02	4.50 ± 0.18
	.25 ± 0.05	1.56 ± 0.07	3.52 ± 0.51	8.04 ± 0.31	.226 ± 0.02	3.87 ± 0.14
JHL-10	.10 ± 0.05	1.70 ± 0.07	3.38 ± 0.51	8.34 ± 0.32	.204 ± 0.02	4.59 ± 0.18
	.25 ± 0.05	1.70 ± 0.07	3.38 ± 0.51	8.34 ± 0.32	.204 ± 0.02	3.95 ± 0.16
JHL-6	.10 ± 0.05	1.56 ± 0.07	3.93 ± 0.51	7.52 ± 0.29	.172 ± 0.02	4.57 ± 0.18
	.25 ± 0.05	1.56 ± 0.07	3.93 ± 0.51	7.52 ± 0.29	.172 ± 0.02	3.92 ± 0.15
JHL-7	.10 ± 0.05	1.85 ± 0.08	4.14 ± 0.59	9.34 ± 0.36	.150 ± 0.02	5.18 ± 0.21
	.25 ± 0.05	1.85 ± 0.08	4.14 ± 0.59	9.34 ± 0.36	.150 ± 0.02	4.44 ± 0.18
JHL-2	.10 ± 0.05	1.86 ± 0.08	3.68 ± 0.61	10.28 ± 0.39	.132 ± 0.01	5.08 ± 0.21
	.25 ± 0.05	1.86 ± 0.08	3.68 ± 0.61	10.28 ± 0.39	.132 ± 0.01	4.35 ± 0.18
JHL-4	.10 ± 0.05	2.00 ± 0.08	3.73 ± 0.62	10.56 ± 0.40	.130 ± 0.01	5.27 ± 0.22
	.25 ± 0.05	2.00 ± 0.08	3.73 ± 0.62	10.56 ± 0.40	.130 ± 0.01	4.51 ± 0.18
JHL-3	.10 ± 0.05	1.99 ± 0.08	3.86 ± 0.59	9.63 ± 0.37	.122 ± 0.01	5.19 ± 0.21
	.25 ± 0.05	1.99 ± 0.08	3.86 ± 0.59	9.63 ± 0.37	.122 ± 0.01	4.45 ± 0.18

B. TL data and ages for loess samples. Listed in stratigraphic order.

Samples[e]	Preheat[f]	Bleach[g]	D_E[h] (Gy)	Temp./time[i]	Age 10% water (ka)[j]	Age 25% water (ka)[j]	Total age range (ka)[j]
JHL-13	140°C/7 h	TB	84.0 ± 1.9	340–380°C	17.6 ± 1.6	20.4 ± 1.9	16–22
	140°C/7 h	PB	84.1 ± 4.6	330–390°C	17.6 ± 2.4	20.4 ± 2.8	
JHL-5	124°C/64 h	TB[k]	106 ± 2.1	360–410°C	23.5 ± 2.1	27.3 ± 2.4	21–30
JHL-10	124°C/64 h	TB[k]	159 ± 4.4	370–410°C	34.7 ± 3.4	40.4 ± 4.0	31–44
JHL-6	124°C/64 h	TB	208 ± 5.5	360–440°C	45.5 ± 4.3	53.0 ± 5.1	41–58
JHL-7	140°C/7 h	TB	237 ± 5.1	200–380°C	45.8 ± 4.2	53.4 ± 5.0	41–58
	140°C/7 h	PB	228 ± 8.2	200–390°C	44.0 ± 4.7	51.3 ± 5.6	
JHL-2	124°C/64 h	TB	344 ± 12	300–440°C	67.7 ± 7.3	79.1 ± 8.6	60–88
JHL-4	124°C/64 h	TB	306 ± 14	200–380°C	*58.1 ± 7.0*[l]	*67.9 ± 8.3*[l]	51–76
JHL-3	140°C/7 h	TB	333 ± 11	240–350°C	*64.1 ± 6.7*[l]	*74.8 ± 8.0*[l]	57–82
	140°C/7 h	PB	315 ± 13	230–350°C	*60.6 ± 7.0*[l]	*70.7 ± 8.2*[l]	

[a] Assumed ratio of weight of water/weight of dry sample, based on measured values as collected and saturation conditions. Uncertainties here and elsewhere are ±1 sigma.
[b] Determined by in-situ gamma spectrometer, count times are approximately 30–35 min at sample site.
[c] Calculated from sample elevation and depth at time of collection as estimated from Prescott and Hutton (1994).
[d] Assumed alpha efficiency value of 1.0 ± 0.2 pGy/m^2 from Berger (1988). Gy = Grays.
[e] The polymineral 4–11 µm size fraction was used for all measurements. For all runs, the heating rate was 5°C/s. TL was detected through Kopp 7–59 and Schott UG-11 filters on a Daybreak Model 1100 Instrument.
[f] Chosen pre-readout annealing temperature and duration.
[g] TB = "total bleach" method from Singhvi et al. (1982) and PB = "partial bleach" method from Wintle and Huntley (1980) with protocol from Berger (1988). Samples run as multiple aliquot additive dose (MAAD). All PB samples exposed to natural sunlight in Denver, CO for one hour before readout and TB residual signal from a 16 hour exposure to natural sunlight in Denver, CO when skies were clear >75% of the exposure.
[h] A weighted saturating exponential regression model was employed for all samples.
[i] The readout temperature for which the D_E is calculated, "plateau" area.
[j] Ages ±2 sigma. Total age range based on minimum with 10% water and maximum with 25% water.
[k] A plateau was either not observed or proved ambiguous and the plateau temperature interval was limited (40–50°C), and begins at a relatively high temperature; thus the corresponding D_E and age values may be only maximum estimates for these samples.
[l] Ages problematic from Bt soil horizons and considered minimum ages (see text).

analysis) and Shannon Mahan (sample analyses, dosimetry, and reporting). TL analyses (Table 1) were undertaken on 4–11 µm mixed mineralogy samples following methods outlined by Aitken (1985), as modified by Millard and Maat (1994) and Maat and Johnson (1996). The protocols used were partial-bleach multiple-aliquot additive dose (PB-MAAD) and total-bleach multiple-aliquot additive dose (TB-MAAD). In situ concentrations of K, U, and Th were determined in the field using a gamma spectrometer, with count times of approximately 30–35 min for each sample.

Water content by volume needs to be estimated to calculate the TL age. For loess, water saturation is ~40–50%, field capacity is half that or ~20–25%, and wilt point is ~10% (Or and Wraith, 1999; John Wraith, soil physicist, Montana State University, oral commun., July, 2002). For comparison, estimates of average water content range from 25% in loess in Belgium (Frechen et al., 2001), 10% in pristine loess, and 20% in B horizons (Singhvi et al., 2001). For sites in Montana similar to the Porcupine Creek section, soil moisture at 1 m is 10% or greater and may average twice that (Farnes, 1978). For the uppermost four TL samples (Table 1A and B) water content may have been closer to 10% than 25% for this is consistent with soil drying indicated by the Bk horizons. For the lowermost accepted two TL samples (Table 1) water content may have averaged closer to ~25% because the soils were mostly moist enough to not develop Bk horizons. We calculated and plotted ages using both 10 ± 5% and 25 ± 5% water by volume and two standard deviations of the TL analysis (Table 1A and B; Figs. 6, 7).

Radiocarbon dating

Radiocarbon ages were obtained from two pits that exposed the Soil 5 mollic A horizon to determine whether they would date near or beyond the limit of ^{14}C dating, as they would if consistent with the TL ages of more than 60 ka. John McGeehin of the U.S. Geological Survey Laboratory in Reston prepared the samples using the humic acid extraction method of McGeehin et al. (2001). These extractions were dated by AMS at the Lawrence Livermore accelerator laboratory.

Cosmogenic ^{10}Be surface exposure dating

In prior work by Licciardi and Pierce (2008), eight boulders were sampled near the Bull Lake glacial limit south of Jackson Hole (Fig. 3) for cosmogenic ^{10}Be surface exposure dating. Excluding one young outlier attributed to boulder rotation or exhumation, the results (n = 7) yield a mean age of 136 ± 13 ^{10}Be ka (± 1 S.D.), as derived using the CRONUS-Earth (Cosmic-Ray prOduced NUclide Systematics on Earth) online ^{10}Be exposure age calculator (http://hess.ess.washington.edu/math) (Balco et al., 2008) when calculated with a boulder surface erosion rate of 1 mm/1000 yr. See Licciardi and Pierce (2008) for age-calculation details. It has been noted in several previous exposure-age studies (e.g., Putkonen and Swanson, 2003; Briner et al., 2005; Kaplan et al., 2005; Putkonen and O'Neil, 2006) that true ages of moraines which have experienced degradation over these timescales are most closely constrained by the oldest boulder exposure ages in the distribution. The reasoning behind this assessment is that most common geologic factors such as erosion, exhumation, and past cover will lead to erroneously young exposure ages, whereas isotope inheritance is comparatively rare. Notably, the two oldest boulder exposure ages obtained from the Bull Lake ice limit (151 ± 2 and 157 ± 2 ka) are within ~6 ka of each other. With the above considerations in mind, here we adopt the midpoint and range of these two ages and their respective uncertainties, 154 ± 5 ka, as the best representation of the Bull Lake moraine age. The outwash gravel at the base of the Porcupine Creek section is correlated with these Bull Lake moraines; hence the age-depth model of the section is anchored to 154 ± 5 ka at its base. We recognize that ongoing and future refinements in cosmogenic ^{10}Be production parameters will inevitably improve the accuracy of the Bull Lake exposure ages, but these future revisions are unlikely to affect the major conclusions of this paper.

Meteoric ^{10}Be analyses

Meteoric ^{10}Be analyses were used to estimate the duration of sedimentation and pedogenesis for loess–soil Units in the lower part of the section that were not suitable for or are beyond the range of TL dating. This method estimates the cumulative duration of sedimentation and pedogenesis in a Quaternary stratigraphic section by measuring the inventory of meteoric ^{10}Be (atoms/cm^2) delivered by precipitation during pedogenesis (Curry and Pavich, 1996; Markewich et al., 1998; 2011). Thus, soils that have longer residence times beneath stable surfaces and have better-developed horizons will also have higher concentrations (atom/g) and inventories (atom/cm^2) of ^{10}Be (see examples in Curry and Pavich, 1996; Markewich et al., 1998; and Muhs et al., 2003).

Extraction of meteoric ^{10}Be from bulk soil and loess samples followed the method outlined by Pavich et al. (1986). A calibrated, dissolved spike of ^{9}Be was added to each ground sample, mixed with $NaCO_3$ and heated to 1200°C in quartz crucibles. The resulting glass beads were processed chemically to extract a purified BeO powder. Ratios of ^{10}Be/^{9}Be in the BeO powders were measured by accelerator mass spectrometry at Lawrence Livermore National Laboratory.

The residence time calculations require assumptions about the delivery rate of ^{10}Be by wet deposition and the concentration of inherited ^{10}Be deposited with the original loess. Soil residence times (Table 3) were calculated by dividing inventories (corrected for inherited ^{10}Be delivered by dust and for radioactive decay) by a delivery rate of 1×10^6 atom/cm^2/yr. This delivery rate, scaled to the present mean annual precipitation, is based on the Maejima et al. (2005) linear relation of meteoric ^{10}Be deposition to rainfall, and the assumption that soil formation in the past occurred under climates at least as humid as the present in Jackson Hole. Because of the relatively long half-life of ^{10}Be (1.36 Ma; Nishiizumi et al., 2007), radioactive decay over the probable time range of consideration (<160 ka) constitutes a minor reduction in soil inventories.

We subtracted "background" concentrations of inherited meteoric ^{10}Be prior to calculating inventories. Because there are few first-cycle sediments on the Earth's surface, the probability is high that some of the measured meteoric ^{10}Be in loess is inherited from a previous period of pedogenesis and surface accumulation. In China, for example, modern dust has ^{10}Be concentrations of 2.7×10^8 atoms/g (Shen et al., 1992), reflecting recycling of ^{10}Be from previous soils. In Illinois, Curry and Pavich (1996) reported possible background values as high as 5.6×10^8 atoms/g for late Quaternary sediments. In central Alaska, Muhs et al. (2003) used the lowest (~0.152×10^8 atoms/g) concentrations of ^{10}Be in unaltered Holocene loess as a measure of the inherited or "background" value for Pleistocene loess. We have meteoric ^{10}Be data only for the lower part of the loess section (Units 4–8; Table 3). We estimated what the background ^{10}Be concentration might be for the Porcupine Creek section at Jackson Hole by examining the concentration of ^{10}Be in the lower part of Unit 4, where only a weak Bw horizon has formed in loess. Because this Unit represents a short period of loess deposition with only minimal soil development, we consider that a value of 4.6×10^8 atoms/g, slightly less than the measured concentration (4.82×10^8 atoms/g), is a reasonable first approximation for "inherited" ^{10}Be. For the mixed gravel and silt (loess) at the base of the section we estimate inherited ^{10}Be to decrease downward from 3.0 to 0.5×10^8 atoms/g as the gravel content increased (Table 3). These values were subtracted from the concentrations in all other horizons prior to calculating residence times.

Results

Stratigraphy of the Porcupine Creek loess section

The base of the section consists of coarse outwash gravel (Fig. 6) which is correlated on the basis of surficial geologic relationships with Bull Lake moraines dated at 154 ± 5 ^{10}Be ka (Licciardi and Pierce, 2008). The loess–soil units occur as a series of eight packages above this outwash gravel (Fig. 6). Unaltered loess is only found at the base of Units 3 and 1; in all other packages, pedogenesis has extended through the entire thickness of the loess.

We present here a brief description of each of the loess–soil units that rest on the underlying terrace gravels (Fig. 6), from base to top and described in more detail in Supplement 1 (Stratigraphy of the Porcupine Creek loess section). The loamy part of Unit 8 is ~0.4 m thick and accumulated on top of and mixed into the terrace gravels below. The Bt horizon of the soil developed in this loess has continuous moderate clay films and a dark brown (7.5YR 3/4 moist) color. The bottom of the lower backhoe pit exposed only 20 cm of the Soil 8 Bk horizon. But nearby, a cemented Bk horizon 110 cm thick is exposed in a landslide headwall scarp in the top of Bull Lake outwash gravel beneath thick loess. This scarp is only 0.6 km north of the Porcupine Creek section and in the same terrace level and soil-forming environment as the section (Fig. 4). On the margins of the same terrace bench, several other exposures of a cemented Bk horizon and/or soil carbonate coats were noted beneath thick loess. Thus, it is apparent that a substantial Bk horizon is present at correlatives of the Soil 8 Bk horizon at the base of the Porcupine Creek section. Because the Bt horizons of Soils 8, 7, and 6 are so thin (total 133 cm), the Bk horizon at the base Porcupine Creek section may be associated with all three soils. Such a depth for a Bk horizon is shown by the modern soil (Soil 1) where the Bk horizon extends from 110 to 200 cm below the top of the soil.

A discontinuous pebble lag marks the contact between Unit 8 and Unit 7. Unit 7 is ~38 cm thick and difficult to recognize as loess, because pedogenesis has extended through its entire thickness. Soil 7 also has a well-developed Bt horizon with continuous moderate clay films, and is dark yellowish-brown (10YR 3/4 moist) and has a pebble-lag layer at the top of Unit 7 that marks its contact with Unit 6. Unit 6 also has a soil developed throughout its 38 cm thickness and has continuous thin clay films on ped surfaces and is dark yellowish-brown (10YR 3/4 moist). Unlike the lower Units a pebble layer is

Table 2
Age estimates based on soil development.

Soil	Soil development	Minimum age span[1]
5	Textural B with clay films	>12
6	Textural B with clay films	>12
7	Textural B with clay films	>12
8	Textural B with clay films and clay mineral alteration	>15

[1] Based on comparison with surface soil that developed over the last ~12 ka and has a marginal textural B horizon and having no clay films observed.

absent and its upper boundary is indicated by a less clay-rich and pedogenic Bw horizon of Unit 5. Soils 8, 7, and 6 all lack recognizable A horizons, which might be explained by truncation forming stone lines, or obliteration as the loess accreted. In contrast, Soil 5, ~103 cm thick, has a dark A horizon (10YR 2/2 moist) underlain by a Bt horizon (10YR 4/3 moist) with clay films over a Bw horizon. The A horizon of Soil 5 is the distinctive marker horizon that was used for correlation between the three backhoe pits. It is dark enough that it may once have qualified as a mollic epipedon. The dark A horizon of Soil 5 defines a clearly horizontal band in and between the lower and middle pits and thus supports a "layer cake" eolian deposition for the underlying Units, 5, 6, 7, and 8.

Unit 4 is 50 cm thick and has a generally weakly developed B horizon throughout it. The upper interval of Unit 4 (548–558 cm) is from an auger sample in the bottom of the upper pit and was originally classified as Unit 3 in the field; we now place this at the top of Unit 4 because the particle-size analysis shows a bulge in clay content (Fig. 6). In the upper pit, Unit 3 is ~203 cm thick and is one of only two units that contain relatively unaltered loess (C horizon) in its lower part. This unaltered loess transitions upward into a Bk horizon, which in turn grades upward into a Bt horizon (10YR 3/4 moist) with thin continuous clay films on ped faces. Unit 2 is ~90 cm thick and has an A/Bw soil profile. Finally, Unit 1 is 255 cm thick and contains, from bottom to top, unaltered loess, a Bk horizon, a Bw horizon, a Bt horizon (10YR 4/3 moist; clay films not observed), and a dark A horizon. Soil 1 constitutes the modern surface soil in this area and is considered to have developed in post-glacial time after about 12 ka. It was originally classified as a Cryoboroll (Young, 1982), and would now be classified as a Haplocryoll.

Chronology of the Porcupine Creek section

The chronology for the Porcupine Creek section (Fig. 7) is based on: 1) the vertical stratigraphic sequence, 2) TL age estimates (multiple aliquot total bleach; Table 1), 3) the median of ~154 ± 5 ^{10}Be ka for the two oldest boulders on Bull Lake moraines correlated with the Bull Lake outwash gravel at the base of the section, 4) the degree of soil development, particularly a Bt horizon, as calibrated by the 12 ka age of deglaciation and the inferred start of development of the surface soil (Table 2), and 5) for the interval from ~76 ka (TL) to ~154 ka (cosmogenic ^{10}Be), the accumulation of meteoric ^{10}Be in Units 6, 7, and 8, (Table 3, Fig. 7).

Table 3
Age interval estimates for older part of Porcupine Creek section based on meteoric ^{10}Be inventory.

Soil # and horizon	Thickness (cm)	Concentration ^{10}Be atom/g x 10^8	Inherited ^{10}Be atom/g x 10^8	Excess ^{10}Be atom/g x 10^8 (=concentration-inherited)	Bulk density g/cm^3 estimated	Excess x bulk density x thickness (^{10}Be atom/cm^2 x 10^8)	Soil packet excess ^{10}B (^{10}Be atom/cm^2 x 10^8)	Soil residence time (1000 yr) at 1.0 x 10^6 atoms (cm2/yr)*
4Bw	19	4.82	4.6	0.22	1.4	5.9	(#4)	
4Bw	17	5.78	4.6	1.18	1.4	28.1	"	
						Subtotal	33.9	3.3
5A1	11	6.76	4.6	2.16	1.4	33.3	(#5)	
5A2	11	5.46	4.6	0.86	1.4	13.2	"	
5Bt1	11	5.26	4.6	0.66	1.5	10.9	"	
5Bt1	11	5.2	4.6	0.6	1.5	9.9	"	
5Bt2	13	5.12	4.6	0.52	1.5	10.1	"	
5Bt2	13	5.47	4.6	0.87	1.5	17.0	"	
5Bt2	12	5.8	4.6	1.2	1.5	21.6	"	
5Bw	11	5.71	4.6	1.11	1.4	17.1	"	
						Subtotal	133.1	13.35
6Bt	10	5.76	4.6	1.16	1.5	17.4	(#6)	
6Bt	13	7.25	4.6	2.65	1.5	51.7	"	
6Bt	12	8.27	4.6	3.67	1.5	66.1	"	
6Bt	13	9.38	4.6	4.78	1.5	93.2	"	
				0		Subtotals	228.3	22.94
7Bt	12	7.89	4.6	3.29	1.5	59.2	(#7)	
7Bt	13	7.8	4.6	3.2	1.5	62.4	"	
7Bt	13	9.8	4.6	5.2	1.5	101.4	"	
						Subtotal	223.0	22.41
8Bt1	21	11.29	4.6	6.69	1.5	210.7	(#*8)	
8Bt2	20	4.56	3	1.56	1.6	49.9	"	
8Bt3	16	3.06	2	1.06	1.7	28.8	"	
8BC	17	1.26	1	0.06	1.8	1.8	"	
8Bk	20	1	1	0	1.9	0.0	"	
8C	5	1.53	0.5	1.03	1.9	9.8	"	
8C	20	0.54	0.5	0.04	1.9	1.5	"	
						Subtotal	302.6	30.49
						Total age span,	Units 6, 7,8	75.84

Inherited ^{10}Be decreases over transition into sandy gravel.
Bulk density increases over transition into gravel.

* *corrected for radioactive decay of ^{10}Be, λ = 5.1 x 10^{-7}yr^{-1}.*

We accept the upper six TL ages (total bleach) because they: 1) are from only slightly weathered soil horizons (C, Bk or Bw), 2) are stratigraphically consistent, and 3) have reasonable TL systematics. Samples from Units 4 and 3 have analytically indistinguishable ages (age range 41–58 and 42–58 ka), but the unaltered loess at the base of loess 3 indicates that deposition rates may have been relatively rapid during this period. Thus, we tentatively accept these two age determinations because the TL age uncertainties (±16 and ±17 ka) are consistent with the known stratigraphic sequence.

Age problems are apparent in the TL analyses of Bt horizons in Units 6 and 7 (Fig. 7). For TL age sampling, loess from Bt horizons was avoided where possible, but the only material available for these two units was from Bt horizons. Unit 8 was not analyzed for TL dating due to its high degree of alteration and weathering. Total-bleach TL ages on Bt horizons in loess–soil Units 6 and 7 (Table 1; Fig. 7) are considered minimum ages. TL age reversals in Pleistocene loess sections, especially loess samples older than ~70 ka, have been reported from other localities as well, including Germany (Frechen, 1999), the Czech Republic (Musson and Wintle, 1994; Frechen et al., 1999), and Hungary (Frechen et al., 1997).

In addition to the general challenge of dating pedogenically modified horizons older than ~70 ka, we suggest another possibility as to why the TL ages from the Bt horizons of Units 6 and 7 might be erroneously young. Animal burrows are common in the Porcupine Creek section, sometimes to a depth of a meter or more below the modern soil or top of a buried soil. The typical animal burrow (krotovina) is filled with soil material from above and thus introduces younger material into a deeper horizon. Although we avoided all recognizable krotovinas, burrows would not be recognized and could have been sampled if: (1) they were filled with material from above by material similar to the surrounding material, or (2) enough soil development occurred after the krotovina filling to obscure original differences. Either of these processes could cause the two lowest TL ages to be too young. The deepest two ages are roughly equivalent to the age of sediment that would come from stratigraphic horizons 0.7 to 1.5 m higher in the loess section (Fig. 7). In sum, we accept, with caution, TL ages in the upper ~7 m, but reject the TL ages for Units 6 and 7.

For Units 6, 7, and 8 we interpolate between the ~76 ka TL age for the base of Unit 5 (Fig. 7) and the 154 ^{10}Be ka for Bull Lake outwash gravels using residence times based on meteoric ^{10}Be inventories. The residence time calculations are presented in Table 3.

The total residence time of 76 ka calculated for units 6, 7, and 8 (Table 3) is essentially equivalent to the 78 ka interval based on the independently determined age span between the ~76 TL age for the base of Loess 5 and the 154 ^{10}Be ka age for the Bull Lake outwash gravel. The close correspondence between the correlated ^{10}Be age of the Bull Lake outwash gravel and the projected age of the section base from meteoric ^{10}Be residence time may be fortuitous given the respective uncertainties in these two independent chronologic methods as well as the ~76 ka TL age determination. However, we consider the concordance of independently derived age constraints from the cosmogenic and meteoric ^{10}Be data to suggest that our age-depth model for the lower part of the Porcupine Creek section is well-supported and reasonable.

While the non-recognition of A horizons for soils in the lower part of the section may indicate a hiatus, the similarity of age-interval estimates suggests little record is missing and that loess deposited between Bull Lake time and the end of late Wisconsin time is well-preserved at this site. The high degree of preservation makes this an important site for paleoenvironmental reconstruction.

Little carbon is preserved in the buried soils, except for the dark mollic A horizon in Soil 5 (see Supplement 2). Radiocarbon ages on humic acid from this horizon of Unit 5 provide a useful test of the TL results. The dark mollic horizon is at the same level in the middle and lower pits, but because of the slope between the two pits, the dark mollic horizon in the lower pit is only half the depth below the ground surface (2.1 m) as it is in the middle pit (4.1 m and 4.2 m). The sample from the shallowest depth (2.1 m, lower pit) yielded an age of 35,730 ± 390 ^{14}C yr BP. Samples from the middle pit where depth below surface was twice as deep yielded ^{14}C ages of 39,910 ± 580 ^{14}C yr BP (4.1 m) and of 39,860 ± 560 ^{14}C yr BP (4.2 m). These ages are near, at, or beyond the upper limit for ^{14}C dating of humic acid in soil. The sample from the shallowest depth (2.1 m) is likely to be the most contaminated, and yielded the youngest age. Because such ages could readily be affected by younger carbon additions of only a fraction of one percent (including humic acid and old roots), we interpret these ^{14}C results as minimum or actual ages. The oldest radiocarbon age (39,910 ^{14}C yr BP converts to a calibrated age of more than 44 cal ka BP (Fairbanks et al., 2005). Fig. 7 (bar and arrow in top of Unit 5) shows the compatibility of TL ages JHL 6, 7, and 2 relative to this minimum-age control. The age-depth plot shows the top of Soil 5 is 57 ka, compatible with a radiocarbon age of more than 44 cal ka BP (Fig. 7).

Sources of loess

Overview

A useful step in any interpretation of paleoenvironmental records in loess–soil sequences is the identification of the source or sources of the sediment. In some cases, loess bodies have clear links to major fluvial sources, such as the Missouri, Mississippi, Illinois, and Ohio rivers in the mid-continent (Bettis et al., 2003; Muhs and Bettis, 2003). Nevertheless, even in the mid-continent there is sometimes evidence of more than one loess source (see Grimley, 2000, for good examples from Illinois). Loess can be derived from glacial or non-glacial sources, and source regions can either be highly localized or distant (reviewed in Muhs and Bettis, 2003). Particle-size and trace-element geochemical data allow some inferences about potential loess sources at the Porcupine Creek section. Because fine-grained loess can travel tens or even hundreds of kilometers, potential sources include distal loess from Idaho (Figs. 1, 2), as well as local glacial outwash sources from the Yellowstone Plateau, the Absaroka Mountains, the Teton Range, or some combination of these sources. For the lower 1 m of section, the older thinner Loesses 6, 7, and 8 may be from more distal sites.

Sedimentological evidence of loess sources

An earlier study showed that Jackson Hole loess could have been derived from local sources by strong katabatic winds from the north (Glenn et al., 1983). This conclusion was based on southward-fining loess along a north-to-south transect in Jackson Hole. In this transect the ratio of coarse (50–20 μm)-to-fine (20–2 μm) silt ranges from about 3.0 in the north to about 1.5 in the south, although the logarithmic trend explains only about a third of the variation. At the Porcupine Creek section, silt content throughout is high, between 55 and 80% (Fig. 6). Ratios of coarse silt (in our analyses, 53–20 μm) to fine silt at Porcupine Creek range from about 1.4 to 3.4, which spans a slightly greater range than loess in the transect of Glenn et al. (1983).

Relative amounts of coarse and fine silt in loess have been used in two ways by sedimentologists. One approach has been to utilize the ratio of coarse-to-fine silt as a measure of wind strength. This technique has been used at single sites to infer relative wind strengths through time in Europe (Vandenberghe et al., 1998; Rousseau et al., 2002) and China (Nugteren et al., 2004). These workers show that coarse-to-fine silt ratios are highest in unaltered loess (when sedimentation rates are also considered to be highest) and are lowest in altered loess or paleosols (when sedimentation rates are considered to be low or nil). Other workers have used abundances of coarse and fine silt to infer loess sources, along transects going away from hypothesized valleys that might have provided silt supplies. Muhs and

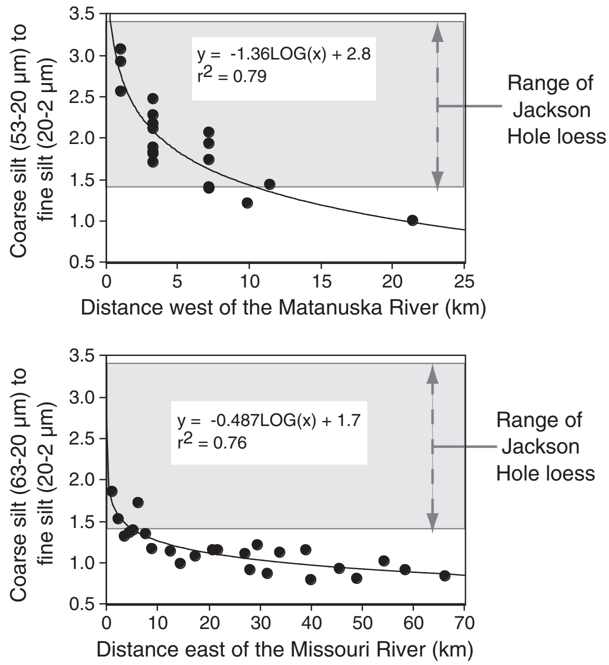

Figure 8. Plots of coarse-to-fine silt in loess as a function downwind from the Matanuska River, Alaska, and the Missouri River, Iowa, showing downwind decrease in particle size. Also shown for comparison on both plots is the range in coarse-to-fine-silt (53–20 μm to 20–2 μm) in the Porcupine Creek section at Jackson Hole (shaded area). Note slight difference in particle size for coarse silt in the Iowa data. Alaska data from Muhs et al. (2004); Iowa data from Muhs and Bettis (2003). Compared to these studies, Wyoming data is compatible with near source (within 10 km).

Bettis (2003) and Muhs et al. (2004) show that coarse silt decreases and fine silt increases with distance from hypothesized source valleys, such as the Missouri and Matanuska Rivers in Iowa and Alaska, respectively (Fig. 8).

Comparison of coarse-to-fine-silt ratios in loess at the Porcupine Creek section with similar data from Iowa and Alaska suggests that loess in Jackson Hole is probably locally derived (Fig. 8). The down-section variability in coarse-to-fine-silt appears to be rather large (Fig. 6), but when viewed from the perspective of distance-decay functions from Iowa and Alaska, the variability is actually not large. In fact, the ratios of coarse-to-fine-silt at Porcupine Creek, which range from about 1.4 to 3.4, are consistent with those for loess that has been transported less than ~10 km from the Matanuska River in Alaska or the Missouri River in Iowa (Fig. 8). We interpret these observations to mean that loess at the Porcupine Creek section was dominantly locally derived, and is not likely to be the distal component of loess from the Palouse region of eastern Washington or perhaps even the Snake River Plain of Idaho (Figs. 1, 2). The ~10 coarse/fine silt peaks (Fig. 6) may represent times of stronger winds.

Geochemical evidence of loess sources

Loess sources can sometimes be identified by mineralogical, isotopic, or geochemical "fingerprinting." Sun (2002a, 2002b) used this approach in identifying loess sources in both the Taklimakan Desert and the Chinese Loess Plateau. Muhs and Budahn (2006) and Muhs and Benedict (2006) used the relative abundance of high-field-strength elements (Ti, Zr, Nb, Y, Cr, Th, and the rare earth elements) in identifying loess sources in Alaska and eolian silt additions to alpine soils in Colorado, respectively. High-field-strength elements are advantageous because they are the least mobile elements in low-temperature, near-surface environments. Thus, even with chemical weathering and pedogenesis, relative abundances of these elements should be affected minimally, if at all. Use of Ti–Zr–Y ternary diagrams to discriminate rock types has a long tradition in igneous petrology, beginning with Pearce and Cann (1973), and has been proven an effective way to discriminate loesses derived from different source sediments (Gallet et al., 1996, 1998; Graham et al., 2001).

To demonstrate the utility of the trace-element fingerprinting approach, we present relative abundances of Ti, Zr, and Y from loess bodies in different regions (Figs. 1, 2, 9). New Zealand loess is probably derived largely from mafic volcanic sources and plots near the Ti apex. Loesses from China, Argentina and Svalbard are derived from somewhat more felsic sources and therefore have somewhat lower Ti and slightly higher Zr. Loess from central Alaska has source sediments that drain metavolcanic rocks with relatively high Ti. In contrast, Nebraska loess is derived from very silicic volcaniclastic rocks and loess from Illinois is derived from Precambrian crystalline rocks and Paleozoic sedimentary rocks. Thus, Nebraska and Illinois loesses have low Ti and high Zr compared to Alaskan loess. These comparisons show that Ti–Zr–Y plots are an effective way to discriminate loesses derived from different source sediments.

Glenn et al. (1983) pointed out that the mineralogy of loess in Idaho is similar to that of loess in Jackson Hole, although they also inferred a local source for Jackson Hole based on particle size data. U–Pb age spectra of detrital zircons from Idaho loess indicate that sources of loess are complex and range from Proterozoic to Tertiary-aged rocks (Link et al., 2005). Furthermore, late Pleistocene and Holocene loesses in Idaho appear to have different sources.

One Ti–Zr–Y comparison we can make is between the Porcupine Creek section and the Tule Island loess section 225 km to the southwest. The Tule Island loess section was exposed in roadcuts before completion of Interstate 86 (42.6156°N, 113.1453°W; Power County, Idaho, Section 26, T9S, R28E). Two overlapping sections were sampled in the roadcut: an upper section ~10 m thick and a lower section ~6.6 m thick. Results indicate that the Tule Island loess section has a Ti–Zr–Y composition intermediate between mafic and felsic rocks (Fig. 9), consistent with the U–Pb zircon data that indicate derivation from a variety of sources. Although Jackson Hole loess also shows a Ti–Zr–Y composition that is intermediate between mafic and felsic rocks, it is distinct from Tule Island loess section (Fig. 9). For both these sections the Ti–Zr–Y plots are for all the soil horizons sampled.

A more likely source for the bulk of the Jackson Hole loess is local glaciogenic silt from the Snake River outwash plains of Jackson Hole, in turn derived from glaciers flowing from the northeast, north, and northwest. Glacial ice from the Yellowstone Plateau and the Absaroka Range traversed volcanic rocks that are distinct in their mineralogy and geochemistry. Rhyolites, which constitute the main rock type in the Yellowstone Plateau (Christiansen, 2001), are relatively enriched in Zr and Y, whereas andesites of the Absaroka Range (Feeley, 2003) are relatively enriched in Ti and Zr, and are depleted in Y. On a Ti–Zr–Y plot, the difference in composition between these two rock types is readily apparent (Fig. 9). However, loess from the Porcupine Creek section falls between the range of values for Absaroka Range andesites and Yellowstone rhyolites. Additional glaciated sources are the Teton Range which is rich in granitic rocks similar to rhyolite, and Mesozoic sedimentary rocks along the east side of Jackson Hole, which are immature and might be similar to the Absaroka andesites. Ice in Jackson Hole came from both the Buffalo Fork and Pacific Creek glacial lobes that traversed Absaroka andesite and Mesozoic sandstone and shale terrain and from the Snake River lobe, which would have traversed Yellowstone Plateau rhyolite terrain (Pierce and Good, 1992; Love et al., 2007). Loess from the upper Snake River Plain remains a possible source.

Evidence of pedogenic alteration

Overview

Particle-size, mineralogical, geochemical, and mineral magnetic data can be used to interpret processes of pedogenic alteration and

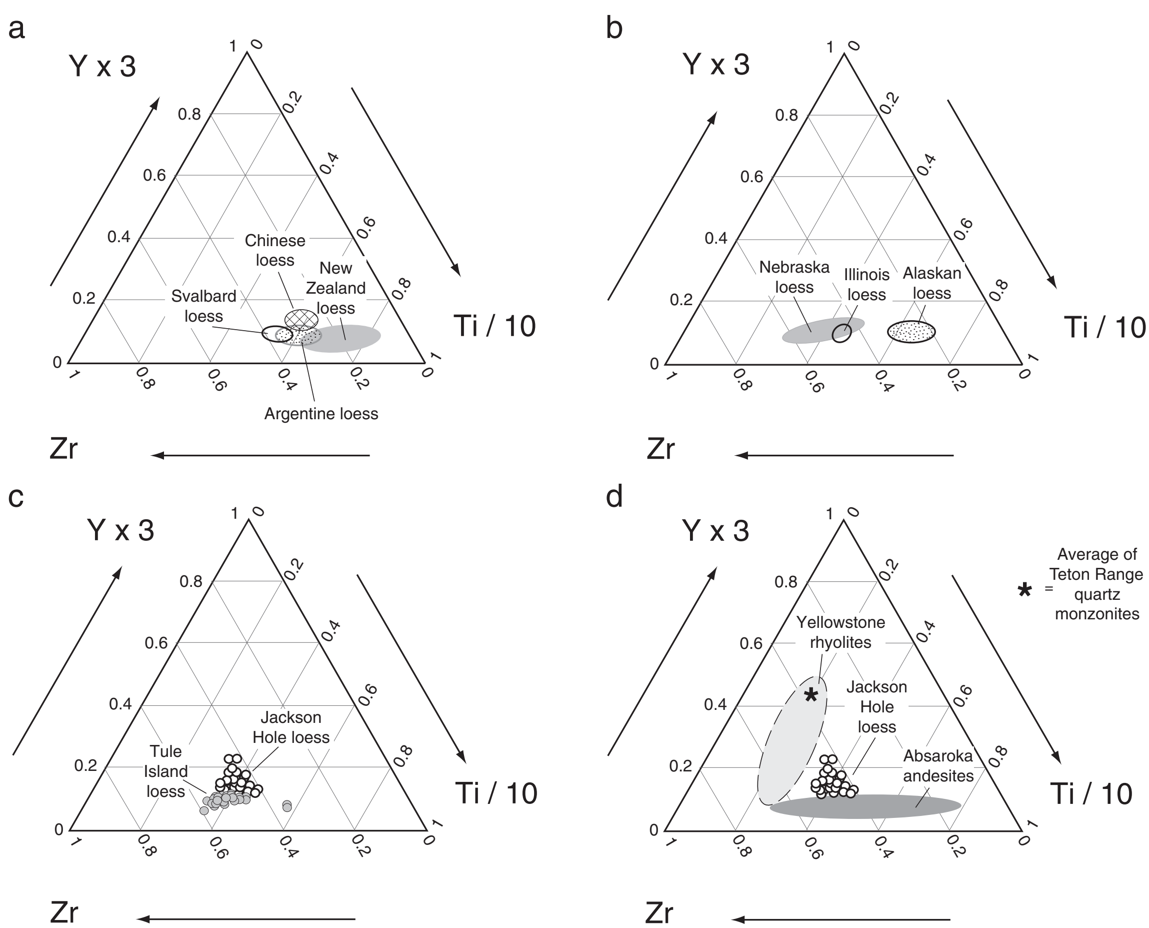

Figure 9. Ternary diagrams showing relative abundance of Ti–Zr–Y for: (a)-various loesses worldwide (Gallet et al., 1996, 1998; Graham et al., 2001); (b)-other loesses in North America (data from Muhs et al., 2008); (c)-the Porcupine Creek loess section (this study) and Tule Island loess, Idaho (this study; we do not have such chemistry for easternmost Idaho loess); and (d) andesites of the Absaroka Range (Feeley, 2003) and rhyolites from the Yellowstone Plateau (Christiansen, 2001).

environments of soil formation in the Porcupine Creek loess section. We summarize these data here and interpret past environments of soil formation in the context of modern processes of soil formation related to current climate and vegetation in the Jackson Hole–Teton Range–Yellowstone Plateau area (Fig. 5).

Soil morphology

One commonly used measure of pedogenesis is the degree of Bt horizon development (Birkeland, 1999). Under climates where there is sufficient rainfall to do so, clay migration can take place when flocculating bivalent cations (Ca^{2+} and Mg^{2+}) have been leached. At the Porcupine Creek section, field evidence of Bt horizon formation is observed in Units 8, 7, 6, 5, 3, and 1 (Fig. 6). This observation is supported by measurements of clay content, which show maxima in nearly all these Bt horizons, but are highest (20–24%) in the Bt horizons of Soils 8, 7, and 3. Bt horizons in Soils 6 and 5 also have clay films, but do not have as distinctive or dramatic a clay "bulge" in the depth profile. Indeed, the Bt horizon in Soil 6 has a low clay content despite field evidence of clay coatings on ped faces.

Because loss of bivalent cations (Ca^{2+} and Mg^{2+}) is normally a prerequisite for clay migration, we would expect to see little evidence of carbonate retained in Bt horizons. Calcium carbonate ($CaCO_3$) was almost certainly a component of the thicker loess units in the Porcupine Creek section at the time of initial deposition of each successive sediment package, because the underlying outwash contains limestone sand and gravel. We measured $CaCO_3$ content in the upper part of the section and CaO and MgO contents in the whole section (Fig. 10). All three geochemical parameters track each other fairly closely. As expected, carbonate content is absent or low in the well developed Bt horizons, although some secondary carbonate was observed on ped faces inferred to have been introduced after soil burial.

As discussed earlier, although for Soil 8 only a Bk horizon only a 20 cm thick was exposed in the bottom of the lower pit, a cemented Bk horizon ~1.1 m thick (petrocalcic horizon) is noted beneath thick loess at the top of Bull Lake gravel 0.6 km to the north (Fig. 4). In a truncated exposure in an abandoned roadcut about 50 m from the lower pit a non-cemented Bk horizon 77 cm thick occurs at the top of the Bull Lake gravel. Consequently, a Soil 8 Bk horizon about 1 m thick in the top of the gravel is correlated in to the base of the section.

In addition to the Bk horizon in the Bull Lake gravels, Soils 3 and 1 have notable zones of pedogenic carbonate accumulation, or Bk horizons below Bt horizons (Fig. 10). These relations suggest that precipitation at the time of soil formation in Soils 3 and 1 was sufficient to leach carbonates out of the upper meter or so of the soil profiles, but insufficient to leach carbonates completely. In contrast, profiles developed in Soils 5 and 4 have little evidence of pedogenic carbonate accumulation or significant amount of original detrital carbonate (Fig. 10), suggesting development under conditions of greater effective moisture. In the Bt horizons of Soils 6 and 7, there are scattered tubular concretions, but the bulk of the Bt horizons do not effervesce and have a very low CaO/TiO_2 ratio (Fig. 10).

Major element geochemistry

Major element geochemistry can be a precise method for assessing the degree of depletion of the main rock-forming minerals in a soil

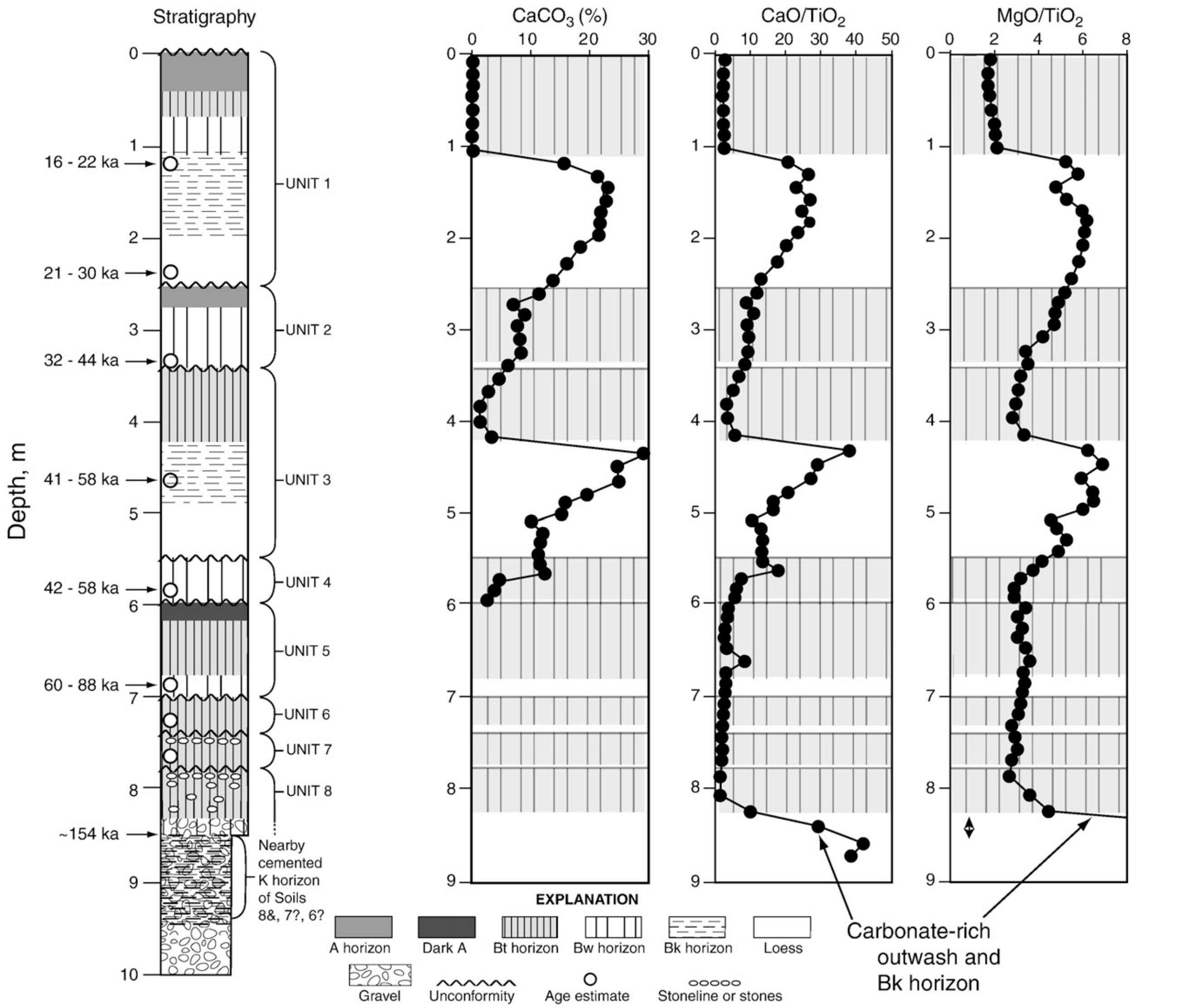

Figure 10. Stratigraphy of the Porcupine Creek loess section and depth plots of $CaCO_3$ content, and ratios of CaO/TiO_2 and MgO/TiO_2 which are measures of carbonate mineral depletion. $CaCO_3$ was not analyzed below 6 m because in Units 5, 6, 7 and the silty part of Unit 8, no primary and only very minor soil carbonate observed as also indicated by plot of CaO/TiO_2 in middle column.

due to pedogenesis and weathering. In loess–paleosol sequences such as those in Jackson Hole, it is useful to normalize the potentially mobile elements to an element of minimal mobility, such as Ti or Zr (Fig. 11). Following the methods used by Muhs et al. (2001, 2008) for loess–paleosol sequences in the Mississippi River Valley and Alaska, we use Ti as an index element for the more-mobile elements K, Na, and P. The major carriers of these minerals are K-feldspar and mica (K), plagioclase and hornblende (Na), and apatite (P). K_2O/TiO_2 does not show depletions that correspond with the best-developed soils. If K-bearing minerals were being depleted in soils, then K_2O/TiO_2 should be lowest in soils and highest in unaltered loess. In fact, the range in variability of this ratio in soils is not much different from the range of variability within unaltered loess, as seen in the basal portion of Unit 3 (Fig. 11). We interpret this to mean that the variability in K_2O/TiO_2 throughout the section mostly reflects variability in the original composition of loess. If there is depletion of K-bearing minerals in the soils, it is masked by the amount of compositional variability in the loess itself. Because both plagioclase and hornblende are susceptible to chemical weathering, we also examined trends of Na_2O/TiO_2 as a function of depth in the section. Depletion in Na is apparent in the lower Bt horizon of Soil 8, lesser depletion of Na in the Bt of Soil 3, and perhaps (only one data point) for the Bw horizon in Soil 2.

For the 2.5 m thick Loess 1, the SiO_2/TiO_2 ratios nearly double from the lower to upper half of Loess 1 (Fig. 11). This is consistent with the change from Pinedale-1 to Pinedale-2 time when a major glacial lobe from the siliceous Yellowstone area was added to the glacial sources for the outwash on the floor of Jackson Hole. The highest SiO_2/TiO_2 ratios in the loess section occur in Loess 5, which also has the highest sand content.

Apatite is the principal carrier of P and of the primary rock-forming minerals; it is second only to olivine in its susceptibility to weathering. Runge et al. (1974), who studied P distribution in loess–paleosol sequences in New Zealand, found that P has a very systematic depth distribution in soils and paleosols as a function of its mobility. Concentrations of P are highest in the upper horizons of soils, where plant cycling has enriched them; lowest in middle-depth soil horizons, where P is depleted either by plant uptake or by downward leaching; and high again in the lowermost soil horizons or uppermost parent material, where neither leaching nor plant uptake have affected the sediment or soil, or where there has been enrichment by leaching from shallower depths. Runge et al. (1974) offered this "high-low-high" pattern of P distribution as a means by which to identify paleosols in loess sections. Muhs et al. (2003) applied the method with some success to verify the presence of paleosols in loess sections of central

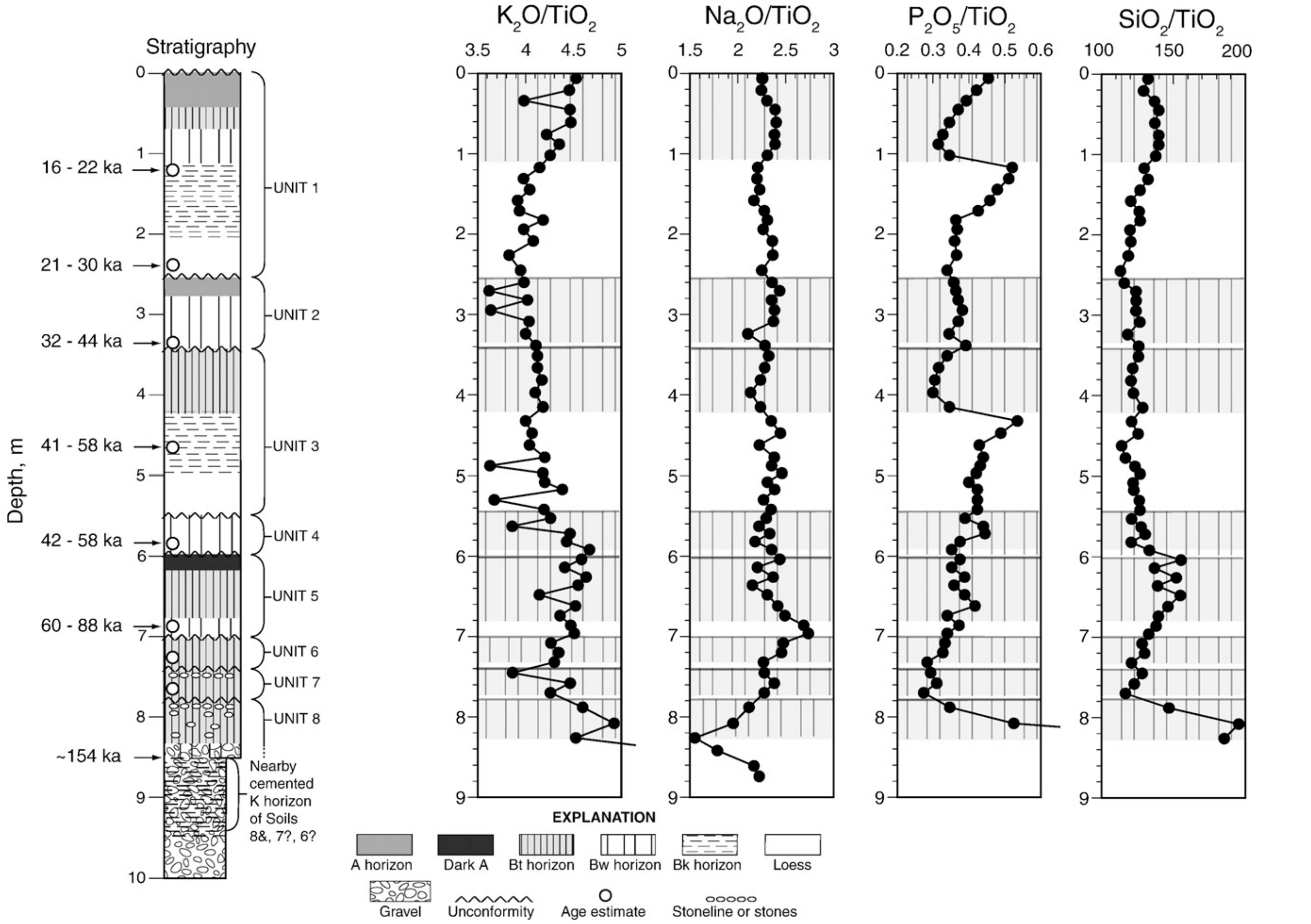

Figure 11. Stratigraphy of the Porcupine Creek loess section and depth plots of K_2O/TiO_2, Na_2O/TiO_2, and P_2O_5/TiO_2, which are measures of silicate mineral depletion. Right column (SiO_2/TiO_2) shows increase in SiO2/TiO_2 in upper half of Loess 1 which is compatible with change in glacial source from east and north east in Pinedale 1 time and from north and northeast in Pinedale 2 time, particularly the siliceous Yellowstone rhyolite Plateau (Fig. 2).

Alaska. In the Jackson Hole loess section (Fig. 11), the modern soil (Soil 1) shows a "high–low–high" pattern of P_2O_5/TiO_2 that is very much like that described by Runge et al. (1974) for soils in loess of New Zealand. A similar pattern is seen with the Unit 3, and possibly a "high–low" pattern in paleosol 4 where there is no Bk horizon. The paleosol in Unit 2 and those in Units 5, 6, 7, and 8 do not show such a clear pattern of P enrichment and depletion.

Mineral magnetic analysis

Mineral magnetic analysis has been applied extensively to Quaternary loess–paleosol sequences especially as a way to recognize the presence of extremely fine-grained ferrimagnetic minerals produced during pedogenesis (see Singer and Verosub, 2007, for a review). In the Porcupine Creek section, variations in magnetic properties (Fig. 12) arise from a variety of factors including dilution by calcite, changes in provenance, and the formation of pedogenic magnetic material. MS and ARM reflect content of ferrimagnetic minerals (i.e., magnetite, titanomagnetite and maghemite) and HIRM largely reflects content of high coercivity magnetic minerals (e.g., hematite). The effects of dilution can be readily observed by comparing the uncorrected values of these parameters to those calculated on a carbonate-free basis (Fig. 12; see Fig. 10 for carbonate percent in upper 6 m). Some of the features in the carbonate-free curves of MS and ARM can be attributed to formation of pedogenic magnetite or maghemite. The most prominent features are the upward increases in MS and ARM in Soil 1. These trends coincide with increases in the presence of superparamagnetic and single-domain ferrimagnetic minerals, indicated by FDMS and ARM/MS, respectively. Such fine-grained ferrimagnetic material is commonly produced by pedogenic processes. Similarly, pedogenic magnetic minerals probably occur in other intervals with elevated values of FDMS and/or ARM/MS (Fig. 12, Soils 1, 3, 5, 6, and 8).

Comparison of carbonate-free magnetic properties to Ti content in zones lacking evidence of pedogenic magnetic minerals (Fig. 13) shows that some variations are due to changes in the mixture of detrital components. Both MS and ARM are highly correlated with Ti-content, with the best-fit line intercepting the Ti axes at 1600 to 1700 ppm. These relations indicate varying mixtures of one component with relatively high contents of ferrimagnetic minerals and Ti and a second component with very low ferrimagnetic mineral content and lower, but significant, Ti content. The first component is probably derived from volcanic rocks of the Yellowstone Plateau and Absaroka Range. The origin of the second component is unknown.

Clay mineralogy

Clay mineralogy is useful in pedologic studies because clay minerals are very sensitive to climatic conditions, vegetation, and duration of pedogenesis (Birkeland, 1999). In the Porcupine Creek loess section, we examined clay minerals in all horizons of the modern soil (Fig. 14) and in the Bt horizons (or Soil 2 Bw horizon) of all the paleosols (Fig. 15). Unaltered loess (Fig. 14; the C horizon of the modern soil) contains abundant smectite, as indicated by a strong peak at 17 Å when glycolated. Upon heating (550°C), this peak disappears and the height of the 10 Å peak increases. Mica is identified by 10 Å and 5 Å peaks (air-dried and glycolated) that remain after heat treatment. The presence of kaolinite is demonstrated by a peak at

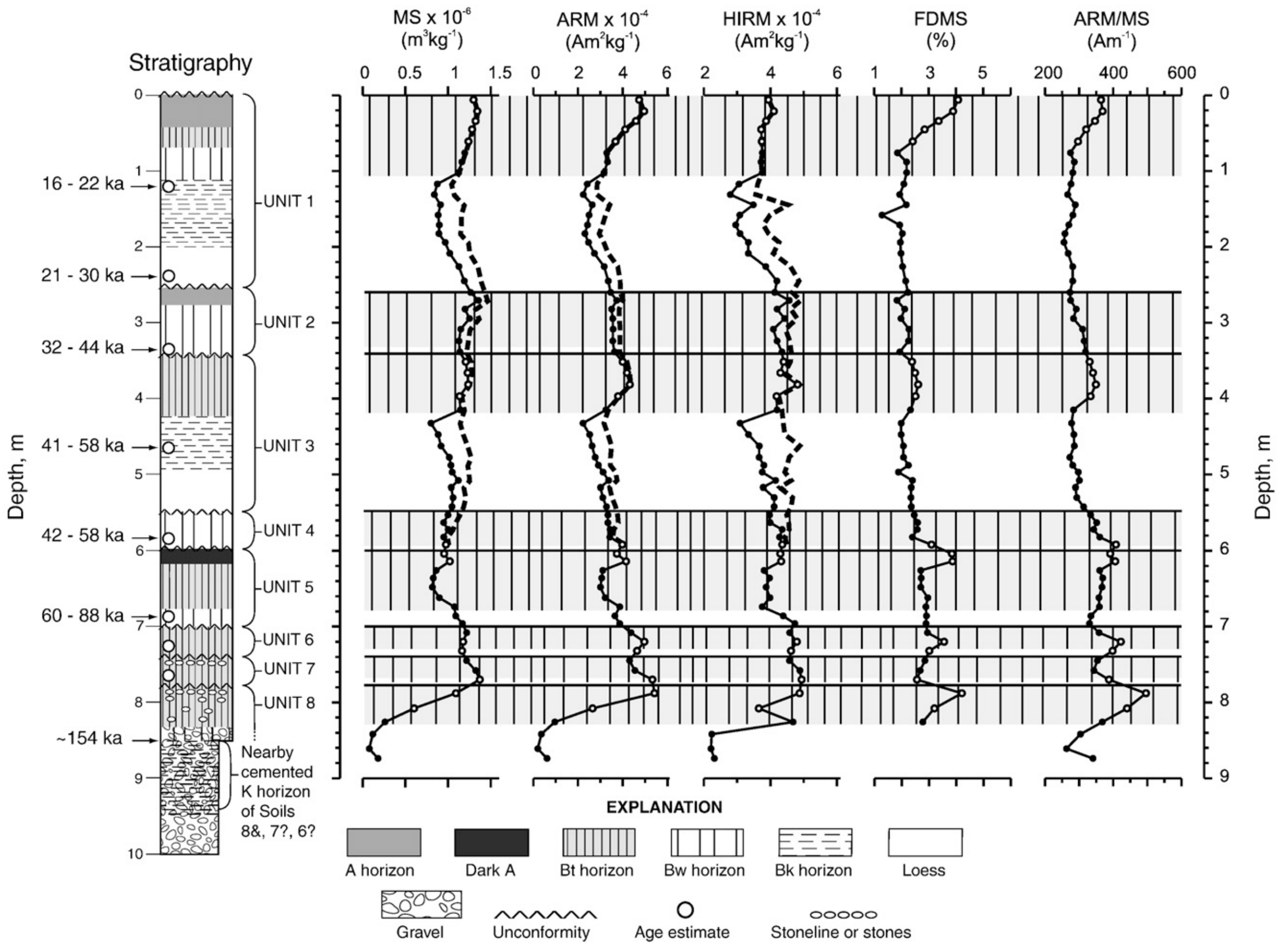

Figure 12. Stratigraphy of the Porcupine Creek loess section and depth plots of magnetic properties: MS (magnetic susceptibility: ferrimagnetic-mineral content); ARM (anhysteretic remanent magnetization: ferrimagnetic-mineral content); HIRM (hard isothermal remanent magnetization; hematite content); FDMS (frequency dependent magnetic susceptibility: ultrafine (superparamagnetic) pedogenic magnetic mineral content); and ARM/MS (very fine (single domain) pedogenic magnetic mineral content). Dashed curves from 0 to 6 m were calculated on a carbonate-free basis. Units 5–8 not corrected for dilution because they had no observed carbonate (see Fig. 10) except for minor secondary carbonate in B horizons and for limestone in gravel. Open symbols indicate samples interpreted to have significant concentrations of pedogenic ferrimagnetic minerals.

7.1 Å (air-dried and glycolated) that disappears after heat treatment, suggesting that the peak at 7.1 Å does not represent chlorite. Clay-sized quartz is also present, as revealed by peaks at 20.0° and 26.6° two-theta; both peaks are unaffected by heat treatment.

In the modern soil (Soil 1), the clay mineralogy in both the Bt and Bw horizons differs little from that of the C horizon, suggesting little pedogenic alteration of the original clay mineral assemblage (Fig. 14). Qualitatively, the same is true for the Bw and Bt horizons of Soils 2 and 3, respectively, (Fig. 15), as smectite, mica, kaolinite, and quartz are all found in these horizons as well. In addition, the relative proportions of these minerals do not look much different from those in the C horizon of the modern soil. In the Bt horizons of Soils 5 and 6, however, the smectite peaks are much broader, shorter, and more asymmetric than those in the younger paleosols, and the kaolinite peaks are relatively

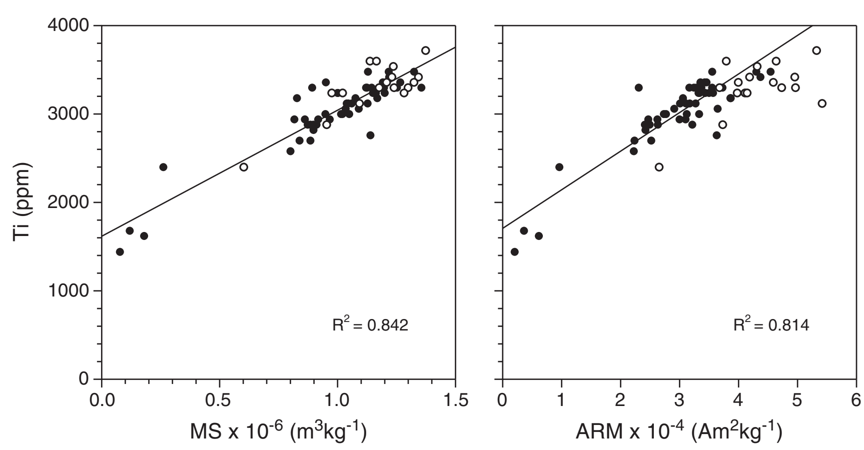

Figure 13. MS (magnetic susceptibility) and ARM (anhysteretic remanent magnetization) versus Ti content. Open symbols indicate samples interpreted to have significant concentrations of pedogenic ferrimagnetic minerals (see Fig. 12), which were not included in calculation of best-fit line.

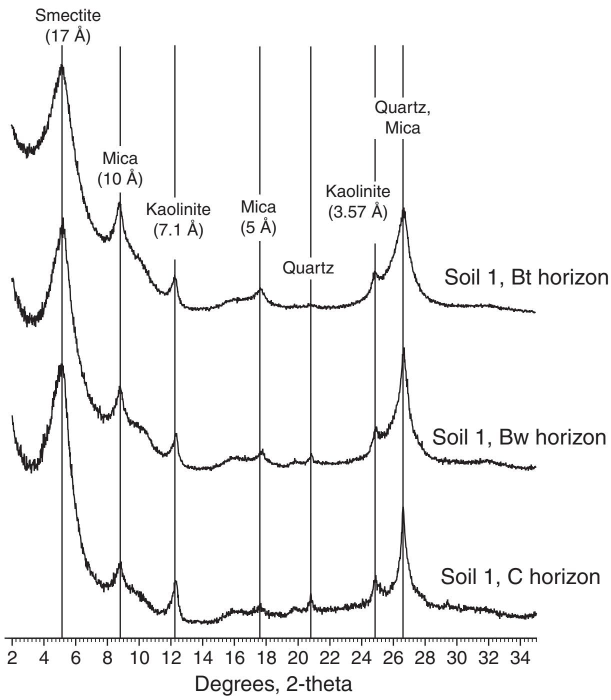

Figure 14. X-ray diffractograms of clay minerals in the Bt, Bw and C horizons of the modern soil (Soil 1) developed in Loess 1. All are glycolated samples. Note that the smectite peak in the Bt horizon is slightly degraded from that in the C horizon.

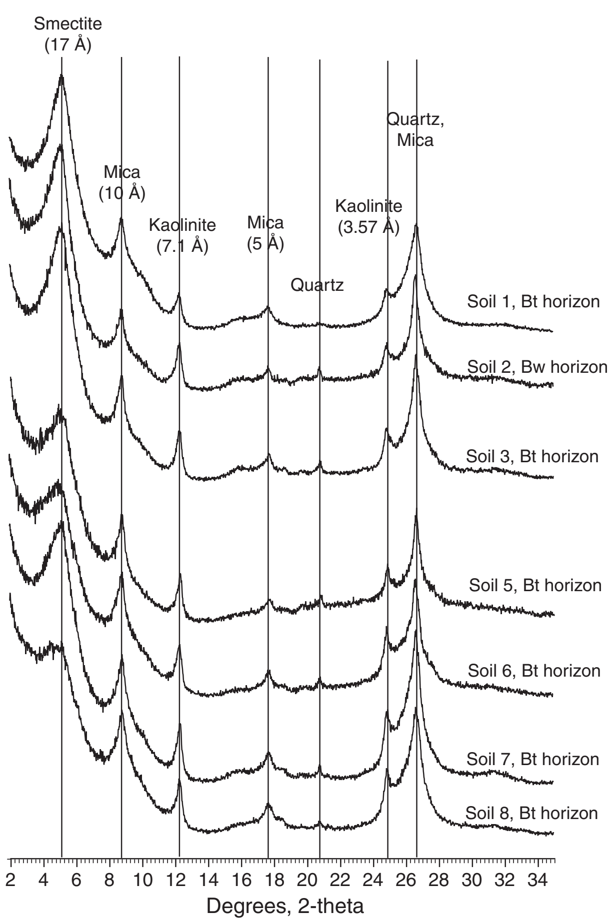

Figure 15. X-ray diffractograms of the clay minerals in Bt horizons from most of the paleosols developed in loess at Jackson Hole, youngest at the top and oldest at the bottom. All are glycolated samples. Note that the smectite peak from Soil 8 is most degraded and that Soils 6 and 5 are also degraded.

higher than Soil 1. These observations suggest possible alteration of smectite to kaolinite or some kind of mixed-layer clay. The Bt horizon of Soil 7, however, has a more prominent smectite peak than in Soils 5 and 6, but a lower smectite peak than the Bt horizons of Soils1, 2, and 3, suggesting minor clay mineral alteration. Finally, the Bt horizon of Soil 8 has the most subdued smectite peak of all suggesting it has the greatest amount of smectite alteration of the entire sequence.

Discussion

Glacial history

The loess–paleosol section at Porcupine Creek contains an unusually complete record of geomorphic events of the past two glacial–interglacial cycles back to ~154 ka (Fig. 16). Outwash at the base of the section is almost certainly of Bull Lake and MIS 6 age, based on its geomorphic position and cosmogenic ^{10}Be surface exposure age of the associated glaciation (Licciardi and Pierce, 2008). Loess 8 is likely a late-stage eolian silt accumulation that was associated with the waning stages of Bull Lake glaciation. Loesses 7 and 6, like Loess 8, are thin, but appear to be discrete accumulations documenting eolian silt deposition, because the paleosols developed in them are distinguishable from each other and are capped by unconformities (Unit 6/5 boundary) as well as stone lines at the boundaries of Units 8/7 and 7/6. If the meteoric ^{10}Be-fallout chronology is reliable, the sequence suggests that Loess 7 and Loess 6 were deposited within the middle and latter part of the last interglacial period (*sensu lato*), possibly correlative with MIS stages 5d and 5b (Fig. 16). Although the thin silts that form Units 6–8 might be from the Snake River Plain, their inclusion in the tight cluster of Ti–Zr–Y-compositions (Fig. 9) with the thicker loesses (Loesses 1–5) is compatible with having roughly the same source as other loesses in the section. Thus, the possibility exists that there may have been periods of minor ice growth in the Yellowstone area during MIS substages 5d and 5b, or alternatively, conditions that were simply more favorable for non-glacial loess deposition. It is not known whether Pleistocene conditions were sufficient to generate katabatic winds from the Yellowstone Plateau, although such winds are not strong under present conditions. In any case, stratigraphic position between ~154 ± 5 ^{10}Be ka Bull Lake outwash gravel and the deepest accepted TL age (roughly 76 ka), as well as the duration intervals indicated by meteoric ^{10}Be buildup, support correlation of the paleosols in Loesses 8, 7, and 6 with the last interglacial period (MIS 5, *sensu lato*).

In particular relevance to Loess 5 and Loess 3, a persistent question in studies of western U.S. glacial history concerns evidence of an earlier Pinedale (i.e., early Wisconsin) ice advance, equivalent in age to MIS 4 and/or early MIS 3 (Colman and Pierce, 1981, 1986; Richmond, 1986; Colman and Pierce,1992; Gillespie and Molnar, 1995; Bischoff and Cummins, 2001; Sharp et al., 2003; Pierce, 2004; Thackray, 2001, 2008). Records bearing on this question include (Fig. 16): 1) the Sierran record of glacial flour during MIS 4 and 3 (Bischoff and Cummins, 2001); 2) glacial flour in a core from Upper Klamath Lake in southern Oregon that extends from the ~37 ka at the base of the core to ~15 ka (Rosenbaum and Reynolds, 2004); 3) the glacial sequence of the Olympic Mountains, Washington, which yields radiocarbon ages in MIS 4? and 3 (Thackray, 2001, 2008); and 4) the glacial sequence near McCall, Idaho, where evidence from weathering rind thicknesses indicates morainal ages correlative with MIS 4 (Colman and Pierce, 1992). Eighty km east of Jackson Hole, pedogenic carbonate on a Wind River outwash terrace started accumulating 55 ± 8.6 ka (Sharp et al., 2003). Based on TL and other age information, Forman et al. (1993) dated an interval of loess deposition on the Snake River Plain between 60 and 80 ka, 150 km west of Jackson Hole. Also to the west near Idaho Falls at a depth of ~5 m down in loess and beneath a weak paleosol, Phillips et al. (2009) obtained an OSL age of

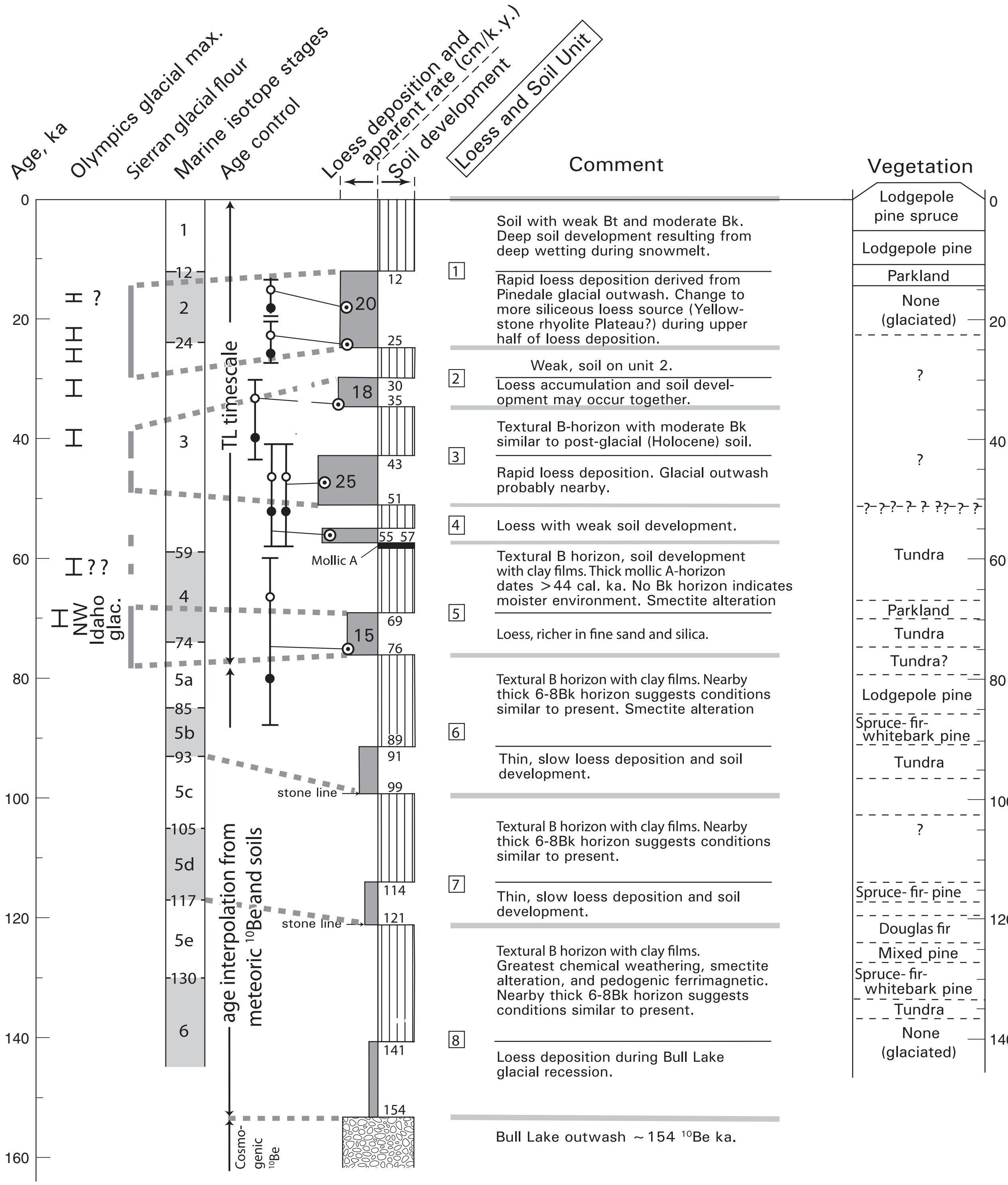

Figure 16. Comparison of several climate records over the last 150 ka. From left to right: 1) Glacial maxima for the Olympic Mountains, WA, (Thackray, 2008)and NW Idaho glaciation (Colman and Pierce, 1986, 1992); 2) Sierran glacial flour (Bischoff and Cummins, 2001), 3) Marine oxygen isotope stages from Martinson et al. (1987); 4) intervals of loess deposition and soil development (this study); 5) comments on loess and soil intervals, and 6) Yellowstone vegetation changes from pollen and plant macrofossils (Baker, 1986). Numbers at changes between loess and soil are ages (in ka) from Fig. 7; these numbers are included for reference only, the actual age uncertainty is probably thousands of years. Loess deposition correlative with MIS 2 and 4 is expectable, but significant and apparently rapid loess deposition at about 40–50 ka, early in MIS 3, is novel. Jackson Hole loess deposition also correlates with Sierran glacial flour during MIS 2 and 4, but during MIS 3 loess deposition dates early and late in MIS 3 whereas Sierran flour dates to the middle of MIS 3. For Yellowstone vegetation, forest intervals tend to correspond to intervals of soil development in the loess section with Douglas fir (the warmest) correlating with Soil 8. Vegetation intervals of tundra or no record generally correlate with loess deposition at the Porcupine Creek section.

75.3 ± 5.2 ka. The Porcupine Creek loess section provides the following evidence of loess deposition and possible glaciation during both MIS 4 and 3.

Loess 5 is a meter thick and topped by the distinctive mollic A horizon. If our combined TL, cosmogenic ^{10}Be, and meteoric ^{10}Be age estimates are reliable, then Loess 5 was deposited in the ~76 to ~69 ka range and correlates with MIS 4 (Figs. 7, 16). Loess 5 has the highest sand content (~25%), but such coarsening is not reflected in the high coarse-fine silt ratio (Fig. 6). High SiO_2/TiO_2 ratios suggest derivation of Loess 5 from a more siliceous source, most likely either: 1) loess derived from outwash from glaciation of the siliceous Yellowstone rhyolite Plateau, or 2) eruptions of ash associated with rhyolite eruptions ~70 ka (Christiansen, 2001).

Loess 4 is 50 cm thick with a weakly to moderately developed soil, and may represent loess deposition combined with soil development. It is treated here as a separate unit, particularly because of a systematic increase in clay to 12.5% at its top.

Loess 3 was deposited ~51–43 ka based the TL ages and soil development (Fig. 7), and thus indicates correlation with an earlier part of MIS 3 (Fig. 16). Loess 3 is about as thick as Loess 1 and appears to represent a significant glacial interval. If glaciation occurred at this time, associated moraines probably have been overridden and obliterated by ensuing Pinedale advances.

Loess 2 was deposited from ~35–30 ka (Fig. 7), and may represent an interval of combined loess deposition and soil development, apparently in the later part of MIS 3.

Loess 1 at Porcupine Creek (~25–12 ka) correlates well with Pinedale ice advances in Greater Yellowstone, and the Teton and Wind River Ranges, particularly in light of cosmogenic nuclide ages of Pinedale end moraines (Gosse et al., 1995; Phillips et al., 1997; Licciardi and Pierce, 2008). This age is similar to dating of the upper loess unit further west. About 100 km to the west near Idaho Falls, Phillips et al. (2009) bracketed upper loess deposition by OSL dating between ~24 ka and ~16 ka. And west of Idaho Falls near the middle of the Snake River Plain, Forman et al. (1993) obtained TL ages of 25 ± 3 ka and 28 ± 3 ka on the middle part of the upper loess unit. Finally, the modern soil in Loess 1 records a significant period of stability in post-glacial time, and probably includes all of the Holocene.

In summary, by their similarity with a Pinedale age for Loess 1, we conclude that both Loess 3 and Loess 5 probably represent "earlier Pinedale" glacial episodes. Our TL ages indicate that Loess 3 could be as old as ~60 ka. However, even with this maximum limiting age, the chronology suggests that a glacial episode represented by Loess 3 would have occurred during the equivalent of MIS 3, rather than MIS 4, according to the SPECMAP chronology (Fig. 16). If this interpretation is correct, then the sequence at Porcupine Creek would be an example of the asynchronous history of mountain glaciers in the western U.S. compared to large continental ice sheets (Gillespie and Molnar, 1995). The marine oxygen isotope record, such as SPECMAP (Martinson et al., 1987) is primarily a chronology of continental ice volume. Thus, by this line of reasoning, global ice volume was greater in MIS 4 than it was in MIS 3, whereas mountain glaciers in Jackson Hole were likely larger in MIS 3 than in MIS 4. In addition, the relationship between loess thickness and glaciation is uncertain; other factors such as vegetation, winds, and dryness are probably involved.

Soil and other paleoenvironmental interpretations

The nature of both the paleosols as well as the loess deposits discussed above in the Porcupine Creek section allow some inferences to be made about paleoclimates in the Jackson Hole region over the course of the past two glacial–interglacial cycles. A useful analog is how modern soils of the area vary as a function of climate and vegetation (Fig. 5). Modern soils in the area that formed under grassland and sagebrush are Agricryolls or Haplocryolls with weakly developed Bt or Bw horizons in their upper parts and Bk horizons in their lower parts. In contrast, soils that formed under forest are Haplocryalfs or Glossocryalfs with better-developed Bt horizons and no Bk horizons.

In the Porcupine Creek section, the modern soil developed in Loess 1 is a good example of a soil that developed under grassland and sagebrush vegetation. Although clay films are not observed in the Bt horizon of this soil, a modest increase in clay content occurs compared to the A or C horizons (Fig. 6). Snowmelt is sufficient to have leached carbonates to depths of a meter or so, a prerequisite for clay migration and pedogenic carbonates have accumulated below this depth and show considerable enrichment (Fig. 10). Thus, the main expression of pedogenesis in the semiarid climate with deep snowmelt wetting that characterizes grasslands in Jackson Hole is deep leaching and concomitant carbonate accumulation at depth.

Soil 2 has more carbonate than in the Bw or Bt horizons of the modern soil (see Fig. 10). This may be explained by either: 1) leaching that was inhibited by loess deposition and limited soil development duration; or 2) carbonate in 2Bw that is associated with Soil 1. There is an overall decrease in carbonate from 1 to 4.1 m and the carbonate in the Bw horizon of Soil 2 and the upper part of the Bt horizon of Soil 3 may indicate carbonate from Soil 1 and possibly Soil 2 is being translocated into the B horizons of Soils 2 and 3. Soil 3 looks very similar to Soil 1 with a Bt horizon that is mostly carbonate-free, but with a well-developed Bk horizon in its lower part (Figs. 7, 10). As a consequence, we interpret this paleosol to have formed under a vegetation cover other than forest, most likely grassland/sagebrush or possibly a dry tundra. Unfortunately, the vegetation record (Baker, 1986) is incomplete through this time period, but does in part include tundra.

Soil 5 has a dark mollic A horizon and a textural Bt horizon with continuous moderate clay films. Soil 5 has no associated Bk horizon. The Bk horizon of Soil 8 is 2.5 m below the top of Soil 5, well below the depth of carbonate accumulation which is about 1 m in Soils 1 and 3. Soil 5 is the only buried soil with a dark, mollic (?) A horizon which suggests a non-forested, grassland or tundra vegetation. Because it is the only buried soil that now displays a dark A horizon, Soil 5 may indicate an unusual environment such as tundra.

Paleosols 5, 6, 7 and 8, have well-expressed Bt horizons and show evidence of pedogenic clay accumulation (Fig. 6, Supplement 1). With the exception of Soil 8, however, these older paleosols show only modest evidence of chemical weathering based on major element composition (Fig. 11). Nevertheless, clay mineralogical analyses show that the Soils 5, 6, and 8 have likely undergone significant depletion of smectite (Fig. 15), and mineral magnetic analyses show that the older paleosols have, in general, more evidence of enrichment of pedogenic ferrimagnetic minerals (Fig. 12).

Although excavation of the gravel in the lower pit was only deep enough to show 20 cm of Bk horizon in the Bull Lake gravel (8Bk), exposures of this horizon 0.6 km to the north (Fig. 4) document the presence of a cemented Bk horizon about 1 m thick. This exposure and at least six other localities (some shown in Fig. 4) of a Bk horizon in Bull Lake gravel beneath loess indicate a calcic soil is common in this stratigraphic position in the area of the Porcupine Creek section and support interpretation of a soil forming environment similar to the present for Soil 8. Our interpretation of these results is that the Soil 8 and possibly Soil 7 and Soil 6 developed under grassland vegetation.

The chronology we have developed for Soils 6, 7, and 8 permits correlation of the buried soils with the last interglacial period in its broadest sense, i.e., all of MIS 5 (Fig. 16). This period of time could have encompassed as much as ~75 ka of pedogenesis, allowing for the formation of a complex of well-developed soils. During this interval, carbonate was leached, three textural B horizons developed, as well as alteration of clay minerals such as smectite, and formation of secondary products possibly including ferrimagmatic minerals.

The series of paleoenvironmental changes sketched above has generally close agreement with Baker's (1986) reconstruction of vegetation changes over the past two glacial–interglacial cycles in the Yellowstone area (Fig. 16). His reconstruction was based on plant macrofossil and pollen data from a series of sections with lake sediments; chronology was based on K-Ar ages of volcanic materials, radiocarbon ages, and stratigraphic relations with Bull Lake and Pinedale tills. According to Baker (1986), the last interglaciation was complex, with a warmer-than-present period during the peak of the last interglaciation (~125 ka?), followed by a somewhat cooler period, and in turn followed by another relatively warm period (~ 80 ka?). Under these alternations of vegetation and climate, Soils 8, 7, and 6 in Jackson Hole might have formed. Baker (1986) considered the period from ~70 ka to 50 ka to be relatively cold, with a dominance of tundra vegetation. Unit 5 apparently developed during this time. Soil 5 with its mollic A horizon, Bt horizon morphology, and lack of carbonate is compatible with a moist tundra environment. There is no record of vegetation in the Yellowstone or Jackson Hole areas between about 50 ka and 30 ka (Baker, 1986) and our chronology allows for an interpretation of Loess 3 being deposited during this interval. Lack of any vegetation records in the Yellowstone area at this time may mean that the area was covered by earlier Pinedale ice, which would be consistent with our interpretation of Loess 3 as glaciogenic. A brief interstadial period, represented by Soil 2 and Soil 3, might indicate glacial recession, followed by the last-glacial maximum (later Pinedale). Baker (1986) also reported no vegetation records in Yellowstone 20-15 thousand years ago, when the Pinedale ice cap covered the Yellowstone area and valley glaciers occupied the Teton Range (Fig. 3). Our TL ages indicate that Loess 1 was deposited at this time, and it is likely that conditions in Jackson Hole were cold and windy, with glacial outwash plains that were sparsely vegetated. At the close of late Pinedale time, the modern soil in Loess 1 started to form, perhaps briefly under a coniferous forest that changed about 10 ka to a climate as warm and dry as present, based on pollen studies in northern Jackson Hole by Whitlock (1993). The modern sagebrush/grassland environment at the Porcupine Creek site produced the Bk horizon lower in the modern soil profile under conditions of deep snowmelt wetting.

Conclusions

The Porcupine Creek loess section records a history of loess deposition and soil development after Bull Lake glaciers retreated from southern Jackson Hole about 150 ka (Fig. 16). At the end of the last glacial (MIS 6) and during the last interglaciation (*sensu lato*, MIS 5), thin loess accumulated and weathered over three episodes (Units 8, 7, and 6) spanning an interval of ~75,000 years. The greatest weathering occurred in Soil 8 (MIS 5e?), as indicated by clay mineral and formation of pedogenic magnetic minerals.

Following formation of Soil 6, about 1 m of sandy Loess 5 accumulated, probably correlative with MIS 4, and possibly associated with nearby glaciation. Soil 5 developed on Loess 5 and produced a mollic A and Bt horizon but not a Bk horizon, possibly in a cold, relatively moist tundra environment. After a short loess–soil interval (Unit 4), about 2.2 m of Loess 3 accumulated, most likely associated with mountain glaciation. Loess 3 accumulated ~51–43 ka early in MIS 3. Glaciation in the mountains of the western U.S. during MIS 3 is supported (Fig. 16) by the glacial flour record from the Sierra Nevada (Bischoff and Cummins, 2001), and by radiocarbon-dated glacial advances in the Olympic Mountains (Thackray, 2008). The SPECMAP ^{18}O marine record is more than ~60% of the amplitude from full interglacial to full glacial conditions at this time, so significant mountain glaciation is reasonable. About 12–25 ka, ~2.5 m of loess deposition occurred during a time correlative with the main Pinedale glaciation. After ~12 ka, a soil developed in this loess with A, Bt and Bk horizons, but with little evidence of clay alteration under semi arid sagebrush–grassland vegetation. Figure 16 summarizes this unusually detailed record of eight cycles of loess deposition and soil development over the last 150 ka.

Supplementary materials related to this article can be found online at doi:10.1016/j.yqres.2011.03.006.

Acknowledgments

This study was supported by the Earth Surface Dynamics Program of the U.S. Geological Survey and is a contribution to the "Eolian History of North America" project (http://esp.cr.usgs.gov/info/eolian/). Our sincere thanks go to the U.S. Forest Service for permission to sample the Porcupine Creek section. We also thank Paula Maat (then of the U.S. Geological Survey, Denver) for initial TL studies of the section, E.A. Bettis III (University of Iowa) for the particle size data, Gary Skipp (U.S. Geological Survey, Denver) for the clay mineralogy data, Kent Houston for two calcic soil descriptions, and Jack McGeehin (U.S. Geological Survey, Reston) for the radiocarbon analysis. Marith Reheis, Margaret Berry, Suzanna Carrithers, and Linda Pierce provided helpful reviews, Tara Preston helped with tables, and Mary Berger drafted most of the illustrations. John Good (USGS, volunteer) contributed greatly to Jackson Hole field studies.

References

Aitken, M.J., 1985. Thermoluminescence Dating. Academic Press, London. 359 pp.
Aleinikoff, J.N., Muhs, D.R., Sauer, R., Fanning, C.M., 1999. Late Quaternary loess in northeastern Colorado, Part II—Pb isotopic evidence for the variability of loess sources. Geological Society of America Bulletin 111, 1876–1883.
Aleinikoff, J.N., Muhs, D.R., Bettis III, E.A., Johnson, W.C., Fanning, C.M., Benton, R., 2008. Isotopic evidence for the diversity of late Quaternary loess in Nebraska: glaciogenic and non-glaciogenic sources. Geological Society of America Bulletin 120, 1362–1377.
Baker, R.G., 1986. Sangamonian (?) and Wisconsinan paleoenvironments in Yellowstone National Park. Geological Society of America Bulletin 97, 717–736.
Balco, G., Stone, J.O., Lifton, N.A., Dunai, T.J., 2008. A complete and easily accessible means of calculating surface exposure ages or erosion rates from ^{10}Be and 26Al measurements. Quaternary Geochronology 3, 174–195.
Berger, G.W., 1988. Dating Quaternary events by luminescence. Geological Society of America, Special Paper 227, 13–50.
Bettis III, E.A., Muhs, D.R., Roberts, H.M., Wintle, A.G., 2003. Last glacial loess in the conterminous U.S.A. Quaternary Science Reviews 22, 1907–1946.
Birkeland, P.W., 1999. Soils and Geomorphology. Oxford University Press, New York. 423 pp.
Bischoff, J.L., Cummins, K., 2001. Wisconsin glaciation of the Sierra Nevada (79,000–15,000 yr BP) as recorded by rock flour in sediments of Owens Lake, California. Quaternary Research 55, 14–24.
Blackwelder, Eliot, 1915, Post Cretaceous history of the mountains of central western Wyoming. Journal of Geology 23, no. 4, 97–117, 193–217, 307–340
Briner, J.P., Kaufman, D.S., Manley, W.R., Finkel, R.C., Caffee, M.W., 2005. Cosmogenic exposure dating of late Pleistocene moraine stabilization in Alaska. Geological Society of America Bulletin 117, 1108–1120.
Busacca, A.J., Begét, J.E., Markewich, H.W., Muhs, D.R., Lancaster, N., Sweeney, M.R., 2004. Eolian Sediments. In: Gillespie, A.R., Porter, S.C., Atwater, B.F. (Eds.), The Quaternary Period in the United States. Elsevier, Amsterdam, pp. 275–309.
Chadwick, O.A., Hall, R.D., Phillips, F.M., 1997. Pleistocene glaciations in the Rocky Mountains: Bull Lake revisited. Geological Society of America Bulletin 109, 1443–1452.
Christiansen, R.L., 2001. The Quaternary and Pliocene Yellowstone Plateau Volcanic Field of Wyoming, Idaho, and Montana. U.S. Geological Survey Professional Paper 729 G. 145 pp.
Colman, S.M., Pierce, K.L., 1981. Weathering Rinds on Andesitic and Basaltic Stones as a Quaternary age Indicator, Western United States. U.S. Geological Survey Professional Paper 1210. 56 pp.
Colman, S.M., Pierce, K.L., 1986. The glacial sequence near McCall, Idaho—weathering rinds, soil development, morphology, and other relative-age criteria. Quaternary Research 25, 25–42.
Colman, S.M., Pierce, K.L., 1992. Varied Records of Early Wisconsin Alpine Glaciation in the Western United States Derived from Weathering-Rind Thicknesses. In: Clark, P.U., Lea, P.D. (Eds.), The Last Interglacial–glacial Transition in North America: Geological Society of America Special Paper 270, pp. 269–278.
Curry, B.B., Pavich, M.J., 1996. Absence of glaciation in Illinois during marine isotope stages 3 and 5. Quaternary Research 46, 19–26.
Dechert, T.V., McDaniel, P.A., Pierce, K.L., Falen, A.L., Fosberg, M.A., 2006. Late Quaternary Stratigraphy, Idaho National Laboratory, Eastern Snake River Plain, Idaho. Idaho Geological Survey Technical Report 06–1. 17 pp.
Despain, Don G., 1990. Yellowstone Vegetation — Consequences of Environment and History in a Natural Setting. Roberts Rinehart, Boulder, Colo. 239 pp.
Duller, G.A.T., 2004. Luminescence dating of Quaternary sediments: recent advances. Journal of Quaternary Science 19, 183–192.
Dunlop, D., Özdemir, Ö., 1997. Rock Magnetism — Fundamentals and Frontiers. Cambridge University Press, New York, NY. 573 pp.
Fairbanks, R.G., Mortlock, R.A., Chiu, T.C., Cao, Li, Kaplan, A., Guilderson, T.P., Fairbanks, T.W., Bloom, A.L., Grootes, P.M., Nadeau, M.J., 2005. Radiocarbon calibration curve spanning 0 to 50,000 years BP based on paired 230Th/234U/228U and ^{14}C dates on pristine corals. Quaternary Science Reviews 24, 1781–1796.
Farnes, P.E., 1978. Summary of Soil Moisture Measurements for Montana, 1949–1978. Soil Conservation Service, U.S. Department of Agriculture. 113 pp.

Feeley, T.C., 2003. Origin and tectonic implications of across-strike geochemical variations in the Eocene Absaroka volcanic province, United States. Journal of Geology 111, 329–346.
Forman, S.L., Smith, R.P., Hackett, W.R., Tullis, J.A., McDaniel, P.A., 1993. Timing of late Quaternary Glaciations in the western United States based on the age of loess on the Eastern Snake River Plain, Idaho. Quaternary Research 40, 30–37.
Frechen, M., 1999. Upper Pleistocene loess stratigraphy in southern Germany. Quaternary Geochronology (Quaternary Science Reviews) 18, 243–269.
Frechen, M., Horvath, E., Gabris, G., 1997. Geochronology of Middle and Upper Pleistocene loess sections in Hungary. Quaternary Research 48, 291–312.
Frechen, M., Zander, A., Cilek, V., Lozek, V., 1999. Loess chronology of the last interglacial/glacial cycle in Bohemia and Moravia, Czech Republic. Quaternary Science Reviews 18, 467–1493.
Frechen, M., van Vliet-Lanoe, Brigitte, van den Haute, Peter, 2001. The Upper Pleistocene loess record at Harmingnies/Belgium—high resolution terrestrial archive of climate forcing. Palaeography, Palaeoclimatology, Palaeoecology 173, 175–195.
Gallet, S., Jahn, B., Torii, M., 1996. Geochemical characterization of the Luochuan loess–paleosol sequence, China, and paleoclimatic implications. Chemical Geology 133, 67–88.
Gallet, S., Jahn, B., Van Vliet-Lanoe, B., Dia, A., Rossello, E.A., 1998. Loess geochemistry and its implications for particle origin and composition of the upper continental crust. Earth and Planetary Science Letters 156, 157–172.
Gillespie, A.R., Molnar, P., 1995. Asynchronous maximum advances of mountain and continental glaciers. Reviews in Geophysics 33, 311–364.
Glenn, W.R., Nettleton, W.D., Fowkes, C.J., Daniels, D.M., 1983. Loessial deposits and soils of the Snake and tributary river valleys of Wyoming and eastern Idaho. Soil Science Society of America Journal 47, 547–552.
Gosse, J.C., Klein, J., Evenson, E.B., Lawn, B., Middleton, R., 1995. Beryllium-10 dating of the duration and retreat of the last Pinedale glacial sequence. Science 268, 1329–1333.
Graham, I.J., Ditchburn, R.G., Whitehead, N.E., 2001. Be isotope analysis of a 0–500 ka loess–paleosol sequence from Rangitatau East, New Zealand. Quaternary International 76 (77), 29–42.
Grimley, D.A., 2000. Glacial and nonglacial sediment contributions to Wisconsin Episode loess in the central United States. Geological Society of America Bulletin 112, 1475–1495.
Hironaka, M., Fosberg, M.A., Winward, A.H., 1983. Sagebrush–grass Habitat Types of Southern Idaho. University of Idaho Forestry and Range Experiment Station Bulletin 44, 44 pp.
Izett, G.A., Wilcox, R.E., 1982. Map Showing Localities and Inferred Distributions of the Huckleberry Ridge, Mesa Falls, and Lava Creek Ash Beds (Pearlette Family Ash Beds) of Pliocene Age in the Western United States and Southern Canada. U.S. Geological Survey Miscellaneous Investigations Map I-1325.
Kaplan, M.R., Douglass, D.C., Singer, B.S., Ackert, R.P.J., Caffee, M.W., 2005. Cosmogenic nuclide chronology of pre-last glacial maximum moraines at Lago Buenos Aires, 46S, Argentina. Quaternary Research 63, 301–315.
Lamphere, M.A., Champion, D.E., Christiansen, R.L., Izett, G.A., Obradovich, J.D., 2002. Revised ages for tuffs of the Yellowstone Plateau volcanic field: assignment of the Huckleberry Ridge Tuff to a new geomagnetic polarity event. Geological Society of America Bulletin 114, 559–568.
Lewis, G.C., Fosberg, M.A., 1982. Distribution and Character of Loess and Loess Soils in Southeastern Idaho. In: Bonnichsen, Bill, Breckenridge, R.M. (Eds.), Cenozoic Geology of Idaho: Idaho Bureau of Mines and Geology Bulletin, 26, pp. 705–716.
Licciardi, J.M., Pierce, K.L., 2008. Cosmogenic exposure-age chronologies of Pinedale and Bull Lake glaciations in greater Yellowstone and the Teton Range, USA. Quaternary Science Reviews 27, 814–831.
Licciardi, J.M., Clark, P.U., Brook, E.J., Pierce, K.L., Kurz, M.D., Elmore, D., Sharma, P., 2001. Cosmogenic ^{3}He and ^{10}Be chronologies of the northern outlet glacier of the Yellowstone ice cap, Montana, USA. Quaternary Research 29, 1095–1098.
Link, P.K., Fanning, C.M., Beranek, L.P., 2005. Reliability and longitudinal change of detrital-zircon age spectra in the Snake River system, Idaho and Wyoming: an example of reproducing the bumpy barcode. Sedimentary Geology 182, 101–142.
Love, J.D., Reed, J.C. Jr, and Christiansen, A.C., 1992. Geologic Map of Grand Teton National Park. U.S. Geological Survey Miscellaneous Investigations Series Map I-2031, scale 1:62,500.
Love, J.D., Reed Jr., J.C., Pierce, K.L., 2007. Creation of the Teton Landscape, a Geological Chronicle of Jackson Hole and the Teton Range. Grand Teton Natural History Association, Moose, Wyoming. 132 pp.
Maat, P.B., Johnson, W.C., 1996. Thermoluminescence and new ^{14}C age estimates for late Quaternary loesses in southwestern Nebraska. Geomorphology 17, 115–128.
Maejima, Y., Matsuzaki, H., Higashi, T., 2005. Application of cosmogenic ^{10}Be to dating soils on the raised coral reef terraces of Kikai Island, southwest Japan. Geoderma 126, 388–399.
Markewich, H.W., Wysocki, D.A., Pavich, M.J., Rutledge, E.M., Millard Jr., H.T., Rich, F.J., Maat, P.B., Rubin, M., McGeehin, J.P., 1998. Paleopedology plus TL, ^{10}Be, and ^{14}C dating as tools in stratigraphic and paleoclimatic investigations, Mississippi River Valley, U.S.A. Quaternary International 51/52, 143–167.
Markewich, H.W., Wysocki, D.A., Pavich, M.J., Rutledge, E.M., 2011. Age, genesis and paleoclimate interpretation of the Sangamon/Loveland complex in the upper and middle Lower Mississippi Valley, U.S.A. Geological Society of America Bulletin 123, 21–39.
Martinson, D.G., Pisias, G., Hays, J.D., Imbrie, John, Moore, T.C., Shackleton, N.J., 1987. Age dating and the orbital theory of the ice ages: development of a high-resolution 0 to 300,000-year chronostratigraphy. Quaternary Research 27, 1–29.
McGeehin, J., Burr, G.S., Jull, A.J.T., Reines, D., Gosse, J., Davis, P.T., Muhs, D., Southon, J.R., 2001. Stepped-combustion ^{14}C dating of sediment. A comparison with established techniques. Radiocarbon 43, 255–261.
Millard, H.T., Maat, P.B., 1994. Thermoluminescence Dating Procedures in Use at the U.S. Geological Survey, Denver, Colorado. U.S. Geological Survey Open File Report 94–249. 112 pp.
Muhs, D.R., Benedict, J.B., 2006. Eolian additions to late Quaternary alpine soils, Indian Peaks Wilderness Area, Colorado Front Range. Arctic, Antarctic, and Alpine Research 38, 120–130.
Muhs, D.R., Bettis III, E.A., 2003. Quaternary Loess–paleosol Sequences as Examples of Climate-driven Sedimentary Extremes. In: Chan, M.A., Archer, A.W. (Eds.), Extreme Depositional Environments—Mega End Members in Geologic Time: Geological Society of America Special Paper, 370, pp. 53–74.
Muhs, D.R., Budahn, J.R., 2006. Geochemical evidence for the origin of late Quaternary loess in central Alaska. Canadian Journal of Earth Sciences 43, 323–337.
Muhs, D.R., Bettis III, E.A., Been, J., McGeehin, J., 2001. Impact of climate and parent material on chemical weathering in loess-derived soils of the Mississippi River Valley. Soil Science Society of America Journal 65, 1761–1777.
Muhs, D.A., Ager, T.A., Bettis, E.A.I.I.I., McGeehin, J., Been, J.M., Beget, J.S., Pavich, M.J., Stafford Jr., T.W., Pinney, D., 2003. Stratigraphy and paleoclimatic significance of late Quaternary loess–paleosol sequences of the last interglacial–glacial cycle in central Alaska. Quaternary Science Reviews 22, 1947–1986.
Muhs, D.R., McGeehin, J.P., Beann, J., Fisher, E., 2004. Holocene loess deposition and soil formation as competing processes, Matanuska Valley, southern Alaska. Quaternary Research 61, 265–276.
Muhs, D.R., Ager, T.A., Skipp, G., Beann, J., Budahn, J.R., McGeehin, J.P., 2008. Paleoclimatic significance of chemical weathering in loess-derived paleosols of subarctic central Alaska. Arctic, Antarctic, and Alpine Research 40, 396–411.
Musson, F., Wintle, A.G., 1994. Luminescence dating of the loess profile at Dolni Vestonice. Czech Republic: Quaternary Geochronology (Quaternary Science Reviews) 13, 411–416.
Nishiizumi, K., Imamura, M., Caffee, M., Southon, J.R., Finkel, R.C., McAninch, J., 2007. Absolute calibration of ^{10}Be standards. Nuclear Instruments and Methods in Physics Research B 258, 03–413.
Nugteren, Govert, Vandenberghe, Jef, van Huissteden, J.K., Zhisheng, An, 2004. A Quaternary climate record based on grain size analysis from the Luochuan loess section on the central Loess Plateau, China. Global and Planetary Change 41, 167–183.
Or, Dani, Wraith, J.M., 1999. Soil Water Content and Water Potential Relationships. In: Summer, M.E. (Ed.), Handbook of Soil Science. CRC Press, Boca Raton, Florida, pp. A53–A85.
Pavich, M.J., Brown, L., Harden, J.W., Klein, J., Middleton, R., 1986. ^{10}Be distribution in soils from Merced River terraces, California. Geochimica et Cosmochimica Acta 50, 1727–1735.
Pearce, J.A., Cann, J.R., 1973. Tectonic setting of basic volcanic rocks determined using trace element analyses. Earth and Planetary Science Letters 19, 290–300.
Phillips, F.M., Zreda, M.G., Goss, J.C., Klein, Jeffrey, Evenson, E.B., Hall, R.D., Chadwick, O.A., Sharma, Pankaj, 1997. Cosmogenic ^{36}Cl and ^{10}Be ages of Quaternary glacial and fluvial deposits of the Wind River Range, Wyoming. Geological Society of America Bulletin 109, 1453–1463.
Phillips, W.M., Rittenour, T.M., Hoffmann, G., 2009. OSL chronology of late Pleistocene glacial outwash and loess deposits near Idaho Falls, Idaho. Geological Society of America Abstracts with Programs 42 (No. 6), 12.
Pierce, K.L., 1979. History and Dynamics of Glaciation in the Northern Yellowstone National Park Area. U.S. Geological Survey Professional Paper 729F. 91 pp.
Pierce, K.L., 2004. Pleistocene Glaciations of the Rocky Mountains. In: Gillespie, A.R., Porter, S.C., Atwater, B.F. (Eds.), The Quaternary Period in the United States. Developments in Quaternary Science, v. 1. Elsevier Amsterdam, pp. 63–76.
Pierce, K.L., Good, J.D., 1992. Field Guide to the Quaternary Geology of Jackson Hole, Wyoming. U.S. Geological Survey Open-File Report 92–504. 49 pp.
Pierce, K.L., Obradovich, J.D., Friedman, Irving, 1976. Obsidian hydration dating and correlation of Bull Lake and Pinedale glaciations near West Yellowstone. Montana. Geological Society of America Bulletin 87, 703–710.
Pierce, K.L., Fosberg, M.A., Scott, W.E., Lewis, G.C., Colman, S.M., 1982. Loess Deposits of Southeastern Idaho—Age and Correlation of the Upper Two Loess Units. In: Bonnichsen, Bill, Breckenridge, R.M. (Eds.), Cenozoic Geology of Idaho: Idaho Bureau of Mines and Geology Bulletin, 26, pp. 717–725.
Porter, S.C., 2001. Chinese loess record of monsoon climate during the last glacial–interglacial cycle. Earth Science Reviews 54, 115–128.
Prescott, J.R., Hutton, J.T., 1994. Cosmic-ray contribution to dose-rates for luminescence and ESR dating: large depth and long-term time variations. Radiation Measurements 23 (2–3), 497–500.
Putkonen, J.K., O'Neil, M., 2006. Degradation of unconsolidated Quaternary landforms in western North America. Quaternary Research 75, 408–419.
Putkonen, J.K., Swanson, T.W., 2003. Accuracy of cosmogenic ages for moraines. Quaternary Research 59, 255–261.
Richmond, G.M., 1964. Glacial geology of the West Yellowstone Basin and adjacent parts of Yellowstone National Park. U.S. Geological Survey Professional Paper 435T. pp. 223–236.
Richmond, G.M., 1986. Stratigraphy and Correlation of Glaciations in Yellowstone National Park. In: Sibrava, V., Bowen, D.Q., Richmond, G.M. (Eds.), Quaternary Glaciations in the Northern Hemisphere: Quaternary Science Reviews 5, pp. 83–98.
Rieger, Samuel, Juve, R.L., 1961. Soil development in recent loess in the Matanuska Valley, Alaska. Soil Science Society of America Proceedings 25, 243–248.
Rosenbaum, J.G., Reynolds, R.L., 2004. Record of Late Pleistocene glaciation and deglaciation in the southern Cascade Range: II. Flux of glacial flour in a sediment core from Upper Klamath Lake, Oregon. Journal of Paleolimnology 31, 235–252.

Rosenbaum, J.G., Reynolds, R.L., Adam, D.P., Drexler, J., Sarna-Wojcicki, A.M., Whitney, G.C., 1996. Record of middle Pleistocene climate change from Buck Lake, Cascade Range, southern Oregon—evidence from sediment magnetism, trace-element geochemistry, and pollen. Geological Society of America Bulletin 108, 1328–1341.
Rousseau, D.D., Antoine, P., Hatte, C., Lang, A., Zoller, L., Fontugne, M., Othman, D.B., Luck, J.M., Moine, M., Labonne, M., Bentaleb, I., Jolly, D., 2002. Quaternary Science Reviews 21, 1577–1582.
Runge, E.C.A., Walker, T.W., Howarth, D.T., 1974. A study of late Pleistocene loess deposits, South Canterbury, New Zealand. Part I. Forms and amounts of phosphorus compared with other techniques for identifying paleosols. Quaternary Research 4, 76–84.
Scott, W.E., 1982. Surficial Geologic map of the Eastern Snake River Plain and Adjacent Areas, 111° to 115°W. Idaho and Wyoming. U.S. Geological Survey Miscellaneous Investigations Series, Map I-1372, Scale 1:250,000.
Sharp, Warren, Ludwig, K.R., Chadwick, O.A., Amundson, R., Glaser, L.L., 2003. Dating fluvial terraces by 230Th/U on pedogenic carbonate, Wind River Basin, Wyoming. Quaternary Research 59, 139–150.
Shen, C.D., Beer, J., Liu, T.S., Oeschger, H., Bonani, G., Suter, M., Wolfli, W., 1992. ^{10}Be in Chinese loess. Earth and Planetary Science Letters 109, 169–177.
Singer, M.J., Verosub, K.L., 2007. Mineral Magnetic Analysis. In: Elias, S. (Ed.), The Encyclopedia of Quaternary Sciences. Elsevier, Elsevier, Amsterdam, pp. 2096–2102.
Singhvi, A.K., Sharma, Y.P., Agrawal, D.P., 1982. Thermoluminescence dating of sand dunes in Rajasthan, India. Nature 295, 313–315.
Singhvi, A.K., Bluszcz, A., Bateman, M.D., Rao, M.S., 2001. Luminescence dating of loess–palaeosol sequences and coversands: Methodological aspects and palaeoclimatic implications. Earth-Science Reviews 54, 193–211.
Soil Survey Staff, 1993. Soil Survey Manual. Soil Conservation Service. U.S. Department of Agriculture Handbook, p. 18.
Soil Survey Staff, 2010. Keys to Soil Taxonomy, 11th ed. USDA-Natural Resources Conservation Service, Washington, DC. 331 pp.
Sun, J., 2002a. Source regions and formation of loess sediments on the high mountain regions of northwestern China. Quaternary Research 58, 341–351.
Sun, J., 2002b. Provenance of loess material and formation of loess deposits on the Chinese Loess Plateau. Earth and Planetary Science Letters 203, 845–859.
Thackray, G.D., 2001. Extensive early and middle Wisconsin glaciation on the western Olympic Peninsula, Washington, and the variability of Pacific Moisture delivery to the Pacific Northwest. Quaternary Research 55, 257–270.
Thackray, G.D., 2008. Varied climatic and topographic influences on Late Pleistocene mountain glaciation in the western United States. Journal of Quaternary Science 23 (6), 671–681.
Thorson, R.R., Bender, G., 1985. Eolian deflation by ancient katabatic winds: a late Quaternary example from the north Alaska Range. Geological Society of America Bulletin 96, 702–709.
Vandenberghe, J., Huijzer, B.S., Mücher, H., Laan, W., 1998. Short climatic oscillations in a western European loess sequence (Kesselt, Belgium). Journal of Quaternary Science 13, 471–485.
Whitlock, C., 1993. Postglacial vegetation and climate of Grand Teton and southern Yellowstone National Parks. Ecological Monographs 63, 173–198.
Winograd, I.J., Landwehr, J.M., Ludwig, K.R., Coplen, T.B., Riggs, A.C., 1997. Duration and structure of the past four interglaciations. Quaternary Research 48, 141–154.
Wintle, A.G., Huntley, D.J., 1980. Thermoluminescence dating of ocean sediments. Canadian Journal of Earth Sciences 17, 348–360.
Wyoming Geographic Information Science Center, 2007. Yellowstone South quadrangle and Jackson Lake quadrangle, 1: 100,000 land cover mapsavailable at http://www.wygisc.uwyo.edu accessed 13 October 2007.
Young, J.F., 1982. Soil Survey of Teton of Teton County, Wyoming, Grand Teton National Park Area. U.S. Department of Agriculture Soil Conservation Service, Washington, D.C. 173 pp.